CERN-TH/2002-170
MC-TH-2002-03
hep-ph/0207277
July 2002

Higgs-Mediated Electric Dipole Moments in the MSSM: An Application to Baryogenesis and Higgs Searches

Apostolos Pilaftsis[a,b]

[a] *Theory Division, CERN, CH-1211 Geneva 23, Switzerland*
[b] *Department of Physics and Astronomy, University of Manchester, Manchester M13 9PL, United Kingdom*

ABSTRACT

We perform a comprehensive study of the dominant two- and higher-loop contributions to the ^{205}Tl, neutron and muon electric dipole moments induced by Higgs bosons, third generation quarks and squarks, charginos and gluinos in the Minimal Supersymmetric Standard Model (MSSM). We find that strong correlations exist among the contributing CP-violating operators, for large stop, gluino and chargino phases, and for a wide range of values of $\tan\beta$ and charged Higgs-boson masses, giving rise to large suppressions of the ^{205}Tl and neutron electric dipole moments below their present experimental limits. Based on this observation, we discuss the constraints that the nonobservation of electric dipole moments imposes on the radiatively-generated CP-violating Higgs sector and on the mechanism of electroweak baryogenesis in the MSSM. We improve previously suggested benchmark scenarios of maximal CP violation for analyzing direct searches of CP-violating MSSM Higgs-bosons at high-energy colliders, and stress the important complementary rôle that a possible high-sensitivity measurement of the muon electric dipole moment to the level of 10^{-24} e cm can play in such analyses.

PACS numbers: 11.30.Er, 14.80.Er

1 Introduction

The nonobservation of electric dipole moments (EDMs) of the thallium atom and neutron, as well as the absence of large flavour-changing-neutral-current (FCNC) decays put severe constraints on the parameters of a theory. Especially, these constraints become even more severe for supersymmetric theories, such as the MSSM, in which too large FCNC and CP-violating effects are generically predicted at the one-loop level, resulting in gross violations with experimental data. A possible resolution of such FCNC and CP crises, often considered in the literature [1], makes use of the decoupling properties of the heavy squarks and sleptons of the first two generations, whose masses should be larger than ~ 10 TeV. Thus, for sufficiently heavy squarks and sleptons, the one-loop predictions for FCNC and EDM observables can be suppressed up to levels compatible with experiment. Also, such a solution poses no serious problem to the gauge hierarchy, as long as the first two generations of squarks and sleptons are not much heavier than 10 TeV. In this case, because of their suppressed Yukawa couplings, the radiative effect of the first two generations of sfermions on the Higgs-boson mass spectrum is still negligible, when compared to that of TeV scalar top and bottom quarks.[1]

Recently, it has been shown [2, 3] that even third-generation squarks may lead by themselves to observable effects on the electron and neutron EDMs through Higgs-boson-mediated two-loop graphs of the Barr-Zee type [4]. This observation offers new possibilities to probe the CP-violating soft-supersymmetry-breaking parameters related to the third generation squarks. Most interestingly, the same CP-violating parameters may induce radiatively a CP-noninvariant Higgs-sector [5, 6, 7, 8], leading to novel signatures at high-energy colliders [8, 9, 10, 11]. It is then obvious that EDM constraints do have important implications for the phenomenological predictions within the above framework of the MSSM with explicit CP violation. Moreover, employing upper limits on EDMs, one is, in principle, able to derive constraints on the phase of the $\mathrm{SU}(2)_L$ gaugino mass, $m_{\widetilde{W}}$, which plays a central rôle in electroweak baryogenesis [12] in the MSSM [13, 14].

On the experimental side, the current upper limit on the electron EDM d_e, as derived from the absence of a permanent atomic EDM for ^{205}Tl, has improved almost by a factor of 2 over the last few years [15, 16]. Specifically, the reported 2σ-upper limit on a thallium EDM is [16]

$$|d_{\mathrm{Tl}}| \;\lesssim\; 1.3 \times 10^{-24}\; e\,\mathrm{cm}\,. \tag{1.1}$$

[1] One should bear in mind that radiative effects on the neutral Higgs-boson masses are proportional to the fourth power of Yukawa couplings. A simple estimate indicates that the contribution of the second generation of sfermions is at least by a factor of 10^{-7} smaller than those of the third generation.

Then, the electron EDM d_e may be deduced indirectly by means of the effective Lagrangian

$$\begin{aligned}\mathcal{L}_{\rm EDM} \;&=\; -\frac{1}{2}\, d_e\, \bar{e}\, \sigma_{\mu\nu}\, i\gamma_5\, e\, F^{\mu\nu} \;+\; C_S\, \bar{N} N\ \bar{e}\, i\gamma_5\, e \;+\; C_P\, \bar{N}\, i\gamma_5\, N\ \bar{e}\, e \\ &\quad + C_T\, \bar{N}\, \sigma_{\mu\nu}\, i\gamma_5\, N\ \bar{e}\, \sigma^{\mu\nu}\, e \quad + \quad \ldots\,, \end{aligned} \tag{1.2}$$

where C_S, C_P, C_T and the ellipses denote CP-violating operators of dimension 6 and higher. With the aid of the effective Lagrangian (1.2), the atomic EDM of ^{205}Tl may be computed by [17, 18, 19]

$$\begin{aligned} d_{\rm Tl}\, [e\,{\rm cm}] \;&=\; -\,585 \times d_e\, [e\,{\rm cm}] \;+\; 8.5 \times 10^{-19}\, [e\,{\rm cm}] \times C_S\, [{\rm TeV}^{-2}] \\ &\quad -\,8. \times 10^{-22}\, [e\,{\rm cm}] \times C_T\, [{\rm TeV}^{-2}] \;+\; \ldots\,. \end{aligned} \tag{1.3}$$

In (1.3), the dots denote CP-odd operators of dimension 7 and higher. In our analysis, we will assume that like C_T, the CP-odd operators of dimension 7 and higher give rise generically to negligible effects on the ^{205}Tl EDM. Moreover, although the contributions of the neglected CP-odd operators to other heavy atoms may be comparable to that of d_e, the experimental upper limits are still much weaker than $d_{\rm Tl}$, at least by one order of magnitude. Consequently, we will only analyze predictions for the thallium EDM $d_{\rm Tl}$ and consider only two operators: the electron EDM d_e and the CP-odd electron-nucleon operator C_S. From (1.1) and (1.3), it is then not difficult to deduce the following 2σ-upper limits on these two CP-odd operators:

$$|d_e| \;\lesssim\; 2.2 \times 10^{-27}\ e\,{\rm cm}\,, \qquad |C_S| \;\lesssim\; 1.5 \times 10^{-6}\ [{\rm TeV}^{-2}]\,. \tag{1.4}$$

In the MSSM under study, the contributions from d_e and C_S to $d_{\rm Tl}$ can be of comparable size and therefore cannot be treated independently. In fact, depending on their relative sign, one may increase or reduce the EDM bounds on the CP-violating parameters of the theory. Here, the proposed high-sensitivity measurement of the muon EDM d_μ to the level 10^{-24} e cm [20] may offer new constraints complementary to those obtained by $d_{\rm Tl}$, since C_S and all higher-dimensional CP-odd operators are absent.

Unlike the thallium EDM, the upper limit on the neutron EDM d_n is less severe, i.e.

$$|d_n| \;\lesssim\; 1.2 \times 10^{-25}\ e\,{\rm cm}\,, \tag{1.5}$$

at the 2σ confidence level (CL) [21, 22, 23]. Moreover, although promising computations appeared recently based on QCD sum rules [24], the theoretical prediction for d_n is rather model-dependent. For example, the predictions between the valence-quark and quark-parton models may differ even up to one-order of magnitude [25]. Recently, the experimental upper limit on a permanent EDM of the ^{199}Hg atom has been improved by a factor of 4, i.e. $|d_{\rm Hg}| < 2.33 \times 10^{-28}\ e\,{\rm cm}$ at the 2σ CL [26]. On the theoretical side, however, the derivation of bounds [27] from $d_{\rm Hg}$ on the chromoelectric dipole moment (CEDM) operators of u and d quarks contains many uncertainties related to unknown effects of higher-dimensional chiral operators, nucleon-current ambiguities [28], the neglect of the CP-odd three-gluon operator [29, 30], the modeling for extracting the nuclear Schiff moment [19], the s-quark content in heavy nuclei, etc. Thus, we shall not implement mercury EDM constraints in our analysis. Instead, we will consider that no large cancellations [31] below the 10% level occur among the different EDM terms in the neutron EDM. In a sense, such a procedure takes account of a possible complementarity relation [27] between the measurements of the neutron and Hg EDMs.

As we have already mentioned above, in the MSSM one-loop EDM effects [32, 33, 34, 25] can be greatly suppressed below their experimental limits, if the first two generation of squarks and sleptons are made heavy enough, typically heavier than 10 TeV [33]. Within such a framework of the MSSM [35], the dominant contributions to EDMs arise from Higgs-mediated Barr-Zee-type two-loop graphs that involve quarks and squarks of the third generation, charginos and gluinos.[3] In this paper, we improve previous computations of these two-loop contributions to EDMs, by resumming CP-even and CP-odd radiative effects on the Higgs-boson self-energies and vertices [38, 39]. Analogous improvements of higher-order resummation effects are also considered in the computation of the CP-odd electron-nucleon operator C_S. Within the above resummation approach, we compute the original Barr-Zee EDM graph induced by t-quarks beyond the two-loop approximation in the MSSM through one-loop CP-violating threshold corrections to the top-quark Yukawa coupling. Finally, we compute the Higgs-boson two-loop contribution to EDM induced by charginos, and discuss the consequences of the derived EDM constraints on electroweak baryogenesis in the MSSM.

The present paper is organized as follows: in Section 2, we discuss the CP-odd electron-nucleon operator C_S, which gives an enhanced contribution to the thallium EDM $d_{\rm Tl}$ in the large $\tan\beta$ regime [40]. In Section 3, after reviewing the existing dominant

[3] Alternatively, one-loop EDM contributions can be suppressed if the CP phases of the trilinear soft-Yukawa couplings of the first two generations and the CP phases of Wino $\tilde{W}$, Bino $\tilde{B}$ and gluino $\tilde{g}$ are all zero, with $B\mu$ and μ being positive according to our CP conventions. In this case, however, if the first two generations of sfermions are relatively light, e.g. few hundreds of GeV, then additional two-loop EDM graphs [36] exist, such as those induced by a gluino CEDM, which give non-negligible contributions to the EDMs. Furthermore, there are two-loop EDM effects induced by a CP-odd γW^+W^--operator, which do not decouple in the limit of heavy squarks and do not depend on Higgs-boson masses [37]. These two-loop EDM contributions are sub-dominant, yielding an electron EDM term typically smaller than $10^{-27}\ e\,{\rm cm}$.

Higgs-boson two-loop contributions to EDMs, we compute the very relevant Barr-Zee contribution to EDM from t quarks for the first time in the MSSM. In addition, we critically re-examine a very recent calculation [41] on Higgs-boson two-loop EDM effects due to charginos. In Sections 2 and 3, we also improve previous computations of the CP-odd electron-nucleon operator C_S and the electron EDM d_e, by taking properly into account higher-order CP-even and CP-odd resummation effects of Higgs-boson self-energy and vertex graphs. Section 4 is devoted to numerical estimates of EDMs and discusses the impact of the derived EDM constraints on electroweak baryogenesis and on the analysis of direct searches for CP-violating Higgs bosons. Our conclusions are drawn in Section 5.

2 CP-odd electron-nucleon operator C_S

Let us first study the contribution of the CP-odd electron-nucleon operator C_S [17, 18, 19] to the ^{205}Tl EDM. At the elementary particle level, C_S can be induced by two types of CP-odd operators in supersymmetric theories: $\bar{e}i\gamma_5 e\,\bar{q}q$ [40] and $\bar{e}i\gamma_5 e\,\tilde{q}^*\tilde{q}$, where q and $\tilde{q}$ denote quark and squark fields, respectively. In the MSSM, the above two CP-odd operators of dimension 6 and 5 are generated by interactions involving Higgs scalar-pseudoscalar mixing and CP-violating vertex effects, as those shown in Fig. 1.

However, not all quarks and squarks can give rise to potentially large contributions to the ^{205}Tl EDM. Our interest is to consider only enhanced Yukawa and trilinear couplings of the Higgs bosons to quarks and squarks in the decoupling limit of the first two generation of squarks. This criterion singles out the CP-odd operators related to top- and bottom-quarks, and their supersymmetric partners. In fact, as is shown in Fig. 1, heavy quarks and squarks do not contribute directly to the CP-odd operator C_S, but only through the loop-induced Higgs-gluon-gluon couplings, $H_i gg$, after they have been integrated out. Thus, the effective Lagrangian responsible for generating C_S is

$$\mathcal{L}^{(C_S)}_{\rm eff} \;=\; \sum_{i=1}^{3} \frac{g_w\, H_i}{2M_W} \left(g_{H_igg}\, \frac{\alpha_s}{8\pi}\, G^{a,\mu\nu} G^a_{\mu\nu} \;+\; m_e \tan\beta\; O_{3i}\, \bar{e}\, i\gamma_5\, e \right), \qquad (2.1)$$

where $M_W = g_w v/2$, O is the 3×3-mixing matrix that relates the weak to mass eigenstates of the CP-violating Higgs bosons [6, 8], and

$$g_{H_igg} \;=\; \sum_{q=t,b} \left\{ \frac{2}{3}\, g^S_{H_iqq} \;+\; \frac{v^2}{6\, m^2_{\tilde{q}_1} m^2_{\tilde{q}_2}} \Big[(m^2_{\tilde{q}_2} - m^2_{\tilde{q}_1})\, \xi^{(H_i)}_q \;+\; (m^2_{\tilde{q}_1} + m^2_{\tilde{q}_2})\, \zeta^{(H_i)}_q \Big] \right\}. \qquad (2.2)$$

In (2.2), the dimensionless coefficients $g^S_{H_iqq}$, $\xi^{(H_i)}_q$, $\zeta^{(H_i)}_q$, and the stop and sbottom masses are given in the Appendix.

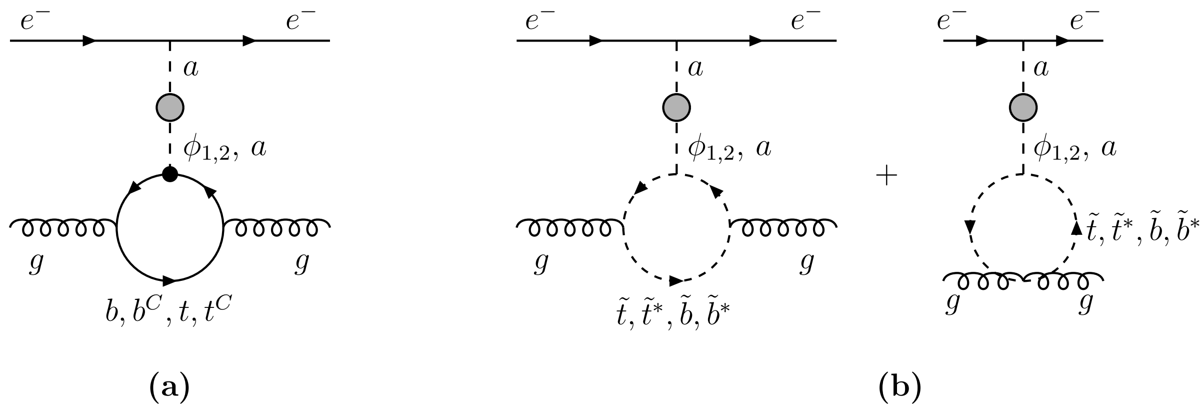

Figure 1: *Feynman graphs contributing to a non-vanishing CP-odd electron-nucleon operator C_S. At the elementary particle level, C_S is predominantly induced by quantum effects involving (a) t-,b- quarks and (b) $\tilde{t}$-, $\tilde{b}$- squarks. Blobs and heavy dots denote resummation of self-energy and vertex graphs, respectively.*

The largest contribution to the coupling parameter $g_{H_i gg}$ comes from the scalar part of the $H_i\bar{b}b$ coupling, $g^S_{H_ibb}$. More explicitly, there are two CP-violating effects that dominate $g^S_{H_ibb}$: (i) the $\tan^2\beta$-enhanced threshold effects [40] described by the term

$$g^S_{H_ibb} \;\sim\; \mathrm{Im}\left[\frac{(\Delta h_b/h_b)\,\tan^2\beta}{1\,+\,(\delta h_b/h_b)\,+\,(\Delta h_b/h_b)\,\tan\beta}\right] O_{3i}\,, \tag{2.3}$$

and (ii) the scalar-pseudoscalar mixing effects contained in the mixing matrix elements O_{1i}. The definition of the quantities $\delta h_b/h_b$ and $\Delta h_b/h_b$ may be found in the Appendix.

At this stage, it is important to observe that if $(\Delta h_b/h_b)\tan\beta \gtrsim 1$, the $\tan^2\beta$-dependence of the CP-violating threshold effects on $g^S_{H_ibb}$ and $g^P_{H_ibb}$ modifies considerably. In particular, in the large $\tan\beta$ limit, $g^S_{H_ibb}$ and $g^P_{H_ibb}$ asymptotically approach a $\tan\beta$-independent constant, i.e.

$$g^S_{H_ibb} \;\;\to\;\; \mathrm{Im}\left[\frac{1\,+\,(\delta h_b/h_b)}{(\Delta h_b/h_b)}\right] O_{3i}\,, \tag{2.4}$$

$$g^P_{H_ibb} \;\;\to\;\; \mathrm{Im}\left[\frac{1\,+\,(\delta h_b/h_b)}{(\Delta h_b/h_b)}\right] O_{1i}\,. \tag{2.5}$$

Although the above limits may only be attainable in a very large $\tan\beta$ and quasi-nonperturbative regime of the theory, the onset of a $\tan\beta$-independent behaviour in $g^S_{H_ibb}$ and $g^P_{H_ibb}$ may already start from moderately large values of $\tan\beta$, i.e. for $\tan\beta \gtrsim 30$. Consequently, the limits (2.4) and (2.5) should be regarded as upper bounds on the CP-violating threshold-enhanced parts of the coupling parameters $g^S_{H_ibb}$ and $g^P_{H_ibb}$. In our numerical analysis in Section 4, we properly take into account the above-described CP-violating resummation effects on $g^S_{H_ibb}$.

The computation of the CP-odd electron-nucleon operator C_S can now be performed by utilizing standard QCD techniques based on the trace anomaly of the energy-momentum tensor [42]. In the chiral quark mass limit, we then have the simple relation

$$\langle N|\,\frac{\alpha_s}{8\pi}\,G^{a,\mu\nu}G^a_{\mu\nu}\,|N\rangle \;=\; -\,(100\text{ MeV})\,\bar{N}N\,. \tag{2.6}$$

With the help of (2.6), we can evaluate the effective $H_i\bar{N}N$-couplings, and hence the CP-odd operator C_S:

$$C_S \;=\; -\,(0.1\text{ GeV})\,\tan\beta\,\frac{m_e\pi\alpha_w}{M_W^2}\,\sum_{i=1}^{3}\frac{g_{H_igg}\,O_{3i}}{M^2_{H_i}}\;. \tag{2.7}$$

Observe that the operator C_S exhibits an enhanced $\tan^3\beta$ dependence [40] and therefore it becomes very significant for intermediate and large values of $\tan\beta$. Numerical estimates for this contribution to a thallium EDM will be presented in Section 4.

3 Higgs-boson two-loop contributions to d_e

We now turn our attention to Higgs-boson two-loop effects [2, 3] on the electron EDM analogous to those first discussed by Barr and Zee [4] in non-supersymmetric theories. As is shown in Fig. 2, these two-loop EDM effects originate predominantly from graphs that involve: stop- and sbottom- squarks (Fig. 2(a,b)) [2], top- and bottom- quarks (Fig. 2(c)), and charginos (Fig. 2(d)) [41].

Strictly speaking, the original Barr-Zee graphs induced by top- and bottom- quarks in Fig. 2(c) appear beyond the two-loop approximation in the MSSM. However, it is a formidable task to analytically compute the complete set of the relevant three- and higher-loop graphs. Therefore, we consider only a subset of higher-loop corrections, in which the dominant CP-violating terms in the Higgs-boson propagators and the Higgs-quark-quark vertices are resumed. Such an approach should only be viewed as an effective one, which is expected to capture the main bulk of the higher-order effects. In the same vein, we improve previous two-loop EDM calculations related to third generation squarks [2] and charginos [41] by resumming dominant CP-violating self-energy terms in the Higgs-boson propagators.

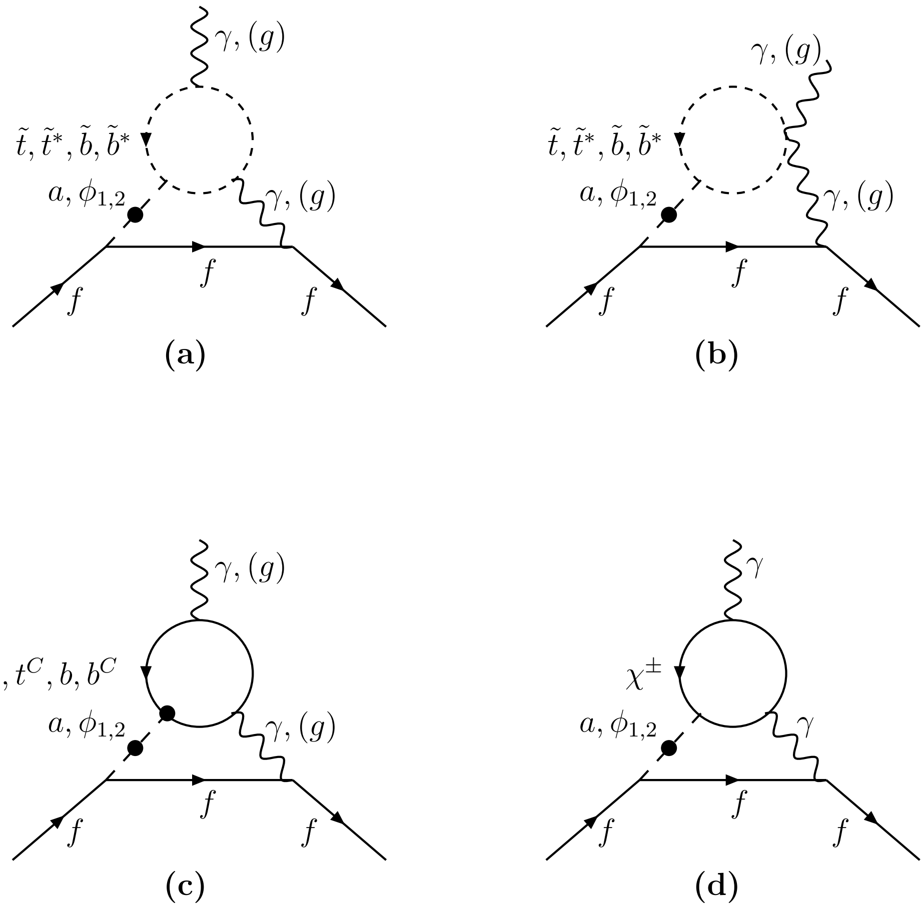

Figure 2: *Dominant Higgs-boson two-loop contributions to EDM of a light fermion $f = e, \mu, d$ in the MSSM with explicit CP violation (mirror-symmetric graphs are not displayed). Heavy dots indicate resummation of self-energy and vertex graphs. Two-loop graphs generating a CEDM for a d-quark are also shown.*

In the context of the aforementioned resummation approach, the dominant Higgs-boson two-loop contributions to electron EDM are individually found to be

$$\begin{aligned}
\left(\frac{d_e}{e}\right)_{\rm (a,b)} &= \frac{3\,\alpha_{\rm em}}{32\,\pi^3}\, m_e \sum_{i=1}^{3} \frac{g^P_{H_iee}}{M^2_{H_i}} \sum_{q=t,b} Q_q^2 \Bigg\{ \xi_q^{(H_i)} \left[F\left(\frac{m^2_{\tilde q_1}}{M^2_{H_i}}\right) \ -\ F\left(\frac{m^2_{\tilde q_2}}{M^2_{H_i}}\right)\right] \\
&\quad + \zeta_q^{(H_i)} \left[F\left(\frac{m^2_{\tilde q_1}}{M^2_{H_i}}\right) \ +\ F\left(\frac{m^2_{\tilde q_2}}{M^2_{H_i}}\right)\right]\Bigg\}\,, \qquad (3.1) \\
\left(\frac{d_e}{e}\right)_{\rm (c)} &= -\,\frac{3\,\alpha^2_{\rm em}}{8\,\pi^2\,\sin^2\theta_w}\,\frac{m_e}{M^2_W} \\
&\quad \times \sum_{i=1}^{3}\sum_{q=t,b} Q_q^2 \left[g^P_{H_iee}\, g^S_{H_iqq}\, f\left(\frac{m_q^2}{M^2_{H_i}}\right) \ +\ g^S_{H_iee}\, g^P_{H_iqq}\, g\left(\frac{m_q^2}{M^2_{H_i}}\right)\right], \qquad (3.2) \\
\left(\frac{d_e}{e}\right)_{\rm (d)} &= -\,\frac{\alpha^2_{\rm em}}{8\,\sqrt{2}\,\pi^2\,\sin^2\theta_w}\,\frac{m_e}{M_W} \\
&\quad \times \sum_{i=1}^{3}\sum_{j=1,2} \frac{1}{m_{\chi^+_j}} \left[g^P_{H_iee}\, a_{H_i\chi^-_j\chi^+_j}\, f\left(\frac{m^2_{\chi^+_j}}{M^2_{H_i}}\right) \ +\ g^S_{H_iee}\, b_{H_i\chi^-_j\chi^+_j}\, g\left(\frac{m^2_{\chi^+_j}}{M^2_{H_i}}\right)\right], \qquad (3.3)
\end{aligned}$$

where $g^P_{H_iee} = -\,\tan\beta\, O_{3i}$, $g^S_{H_iee} = O_{1i}/\cos\beta$, and

$$\begin{aligned}
F(z) &= \int_0^1 dx\ \frac{x(1-x)}{z\ -\ x(1-x)}\ \ln\left[\frac{x(1-x)}{z}\right], \qquad (3.4) \\
f(z) &= \frac{z}{2}\int_0^1 dx\ \frac{1\ -\ 2x(1-x)}{x(1-x)\ -\ z}\ \ln\left[\frac{x(1-x)}{z}\right], \qquad (3.5) \\
g(z) &= \frac{z}{2}\int_0^1 dx\ \frac{1}{x(1-x)\ -\ z}\ \ln\left[\frac{x(1-x)}{z}\right] \qquad (3.6)
\end{aligned}$$

are two-loop functions. In (3.1)–(3.3), the coupling coefficients $g^S_{H_iqq}$, $g^P_{H_iqq}$, $a_{H_i\chi^-_j\chi^+_j}$ and $b_{H_i\chi^-_j\chi^+_j}$, and the squark and chargino masses are given in the Appendix. Equation (3.1) takes on the simpler analytic form presented in [2], if only the CP-odd component a of the Higgs bosons is considered in an unresummed two-loop calculation of the EDM. In this case, the coefficients $\zeta^{(H_i)}$ vanish and $\xi_q^{(H_i)}$ simplifies to

$$\xi_q \ =\ R_q\,\frac{\sin 2\theta_q m_q\, {\rm Im}\,(\mu e^{i\delta_q})}{\sin\beta\,\cos\beta\, v^2}\ =\ \frac{R_q}{\sin\beta\cos\beta}\ \frac{2m_q^2\,{\rm Im}\,(\mu A_q)}{v^2\,(m^2_{\tilde q_2} - m^2_{\tilde q_1})}\ , \qquad (3.7)$$

where $\delta_q = \arg(A_q - R_q\mu^*)$, with $R_t\,(R_b) = \cot\beta\ (\tan\beta)$.

In addition to the dominant Higgs-boson two-loop graphs we have been studying here, there are also sub-dominant two-loop EDM diagrams, where the virtual photon is replaced by a Z boson in Fig. 2. Another class of Higgs-boson two-loop graphs involve the coupling of the charged Higgs bosons $H^\pm$ to the photon and the $W^\mp$ bosons [3]. In this case, for example, the graph in Fig. 2 will proceed via charginos and neutralino in the fermionic loop. As has been explicitly shown in [3] for most of the cases, this additional set of graphs give almost one order of magnitude smaller contributions to EDM. Most importantly, their dependence on the CP-violating parameters of the theory is rather closely related to the two-loop EDM graphs depicted in Fig. 2. Thus, suppressing the dominant Higgs-boson two-loop contributions to EDM will automatically lead to a corresponding suppression of this additional set of two-loop graphs. Therefore, in our analysis we neglect the aforementioned set of sub-dominant two-loop graphs.

So far, we have only been studying the electron EDM d_e. The two-loop prediction for the muon EDM d_μ can easily be obtained from d_e by considering the obvious mass rescaling factor $m_\mu/m_e \approx 205$, i.e.

$$d_\mu \;\approx\; 205\, d_e(t, b, \tilde{t}, \tilde{b}, \chi^\pm)\,, \tag{3.8}$$

where the different two-loop EDM contributions are indicated within the parentheses.

On the other hand, the dominant contributions to neutron EDM d_n come from the CEDM of the d quark and CP-odd three-gluon operator [30], which was first discussed by Weinberg [29] in non-supersymmetric multi-Higgs doublet models. In the MSSM, the CP-odd three-gluon operator decouples as $1/m^3_{\tilde{g}}$ and becomes relevant for gluino masses below the TeV scale. The CEDM of the d quark may be obtained from (3.1) and (3.2), if one replaces the colour factor 3 by 1/2, and $\alpha_{\rm em}\, Q_q^2$ by α_s. The computation of the neutron EDM d_n involves a number of hadronic uncertainties, when the EDMs are translated from the quark to hadron level [25]. For example, considering the valence quark model and renormalization-group running effects from the electroweak scale M_Z down to the low-energy hadronic scale Λ_h [3], one may be able to establish an approximate relation between neutron and electron EDMs. Thus, taking the input values for the involved kinematic parameters: $m_d(\Lambda_h) = 10$ MeV, $\alpha_s(M_Z) = 0.12$ and $g_s(\Lambda_h)/(4\pi) = 1/\sqrt{6}$, we find

$$d_n \;\approx\; -10\, d_e(t, \tilde{t}) \;+\; 1.2\, d_e(t, \tilde{t}, \chi^\pm) \;+\; d_n^{3G}\,. \tag{3.9}$$

On the RHS of (3.9), the first and second terms arise from a d-quark CEDM and EDM, respectively, and d_n^{3G} is the contribution to d_n due to CP-odd three-gluon operator. In obtaining (3.9), we have made two additional approximations as well. First, we neglected the contribution of the u-quark EDM d_u to d_n, as it is much smaller than the d-quark EDM d_d for the relevant region $\tan\beta \gtrsim 3$. Second, we ignored the b- and $\tilde{b}$- quantum corrections to d_d and so to d_n. Formulae (3.8) and (3.9) will be used to obtain numerical predictions for the muon and neutron EDMs in the next section.

4 Numerical estimates and discussion

In Sections 2 and 3, we computed the dominant two- and the resummed higher- loop contributions to EDMs that originate from third generation quarks and squarks, and charginos. Based on the derived analytic expressions, we can now analyze numerically the impact of the experimental constraints owing to the nonobservation of thallium and neutron EDMs on the CP-violating parameters of the theory, and hence on electroweak baryogenesis and direct searches for CP-violating Higgs bosons in the MSSM. Moreover, we will present predictions for the muon EDM d_μ and discuss the implications of a possible high-sensitivity measurement of d_μ to the level 10^{-24} e cm for our analyses.

Based on the observation that CP-violating quantum effects on the neutral Higgs sector get enhanced when the product $\mathrm{Im}\,(\mu A_t)/M^2_{\rm SUSY}$ is large [5, 6], the authors in [8, 9] introduced a benchmark scenario, called CPX, in which effects of CP violation are maximized. In CPX, the following values for the μ- and soft-SUSY breaking parameters were adopted:

$$\begin{aligned}
\widetilde{M}_Q &= \widetilde{M}_t = \widetilde{M}_b = M_{\rm SUSY}\,, \qquad \mu = 4M_{\rm SUSY}\,,\\
|A_t| &= |A_b| = 2M_{\rm SUSY}\,, \qquad \arg(A_{t,b}) = 90^\circ\,,\\
|m_{\tilde g}| &= 1\ \mathrm{TeV}\,, \qquad \arg(m_{\tilde g}) = 90^\circ\,,\\
m_{\widetilde W} &= m_{\widetilde B} = 0.3\ \mathrm{TeV}\,.
\end{aligned} \tag{4.1}$$

Without loss of generality, the μ-parameter is chosen to be real. The predictions of CPX showed [9] that even a light neutral Higgs boson with a mass as low as 60 GeV could have escaped detection at LEP2.[3] A recent experimental analysis of LEP2 data confirms this observation [43]. Here, we wish to investigate the compatibility of the CPX scenario with the experimental limits on EDMs. For this purpose, we allow variations in the gluino phase, which enters the Higgs sector at two loops, but keep the A_t phase in (4.1) fixed. In addition, we will present numerical results for EDMs, where the μ-parameter is varied from 100 GeV to $4M_{\rm SUSY}$. Finally, we leave unspecified the phases of the gaugino mass parameters $m_{\widetilde W}$ and $m_{\widetilde B}$. As we will see below, the phase of $m_{\widetilde W}$ is greatly affected by constraints from the electron EDM.

We start our numerical analysis by presenting predictions for the ^{205}Tl EDM $d_{\rm Tl}$ that arise entirely due to the CP-odd electron-nucleon operator C_S and are denoted as $d_{\rm Tl}(C_S)$. In Fig. 4, we display numerical estimates for $d_{\rm Tl}(C_S)$ as functions of $\tan\beta$ for four different versions of the CPX scenario with $M_{\rm SUSY} = 1$ TeV: (a) $M_{H^+} = 150$ GeV,

[3] Similar remarks were made earlier in [6], but the LEP2 data were less restrictive at the time of writing.

$\arg(m_{\tilde{g}}) = 0°$; (b) $M_{H^+} = 300$ GeV, $\arg(m_{\tilde{g}}) = 0°$; (c) $M_{H^+} = 150$ GeV, $\arg(m_{\tilde{g}}) = 90°$; (d) $M_{H^+} = 300$ GeV, $\arg(m_{\tilde{g}}) = 90°$. The individual $b, \tilde{t}, t, \tilde{b}$ contributions to $d_{\rm Tl}(C_S)$, along with their relative signs, are indicated by different types of lines. We observe that the biggest contribution to $d_{\rm Tl}$ comes from the b- quarks for large values of $\tan\beta$, i.e. for $\tan\beta \gtrsim 15$, for which the CP-violating vertex effects become important (see also discussion in Section 2). In particular, these CP-violating threshold effects, which crucially depend on the term $\mathrm{Im}\,(\Delta h_b/h_b)\,\tan^2\beta$ in (2.3), become even more important for large gluino phases. Thus, the predictions for $d_{\rm Tl}(C_S)$ in panels 4(a) and (b), with $\arg(m_{\tilde{g}}) = 0°$, are one order of magnitude larger than the ones in (c) and (d), with $\arg(m_{\tilde{g}}) = 90°$.

For intermediate and smaller values of $\tan\beta$, i.e. for $\tan\beta \lesssim 15$, CP-violating self-energy effects are significant, especially for relatively light charged Higgs bosons with masses in the range 150–200 GeV. In fact, these effects have generically opposite sign than those due to the CP-violating vertex effects, giving rise to natural cancellations among the contributing EDM terms, and so lead to smaller values of $d_{\rm Tl}(C_S)$. Although our numerical results are in qualitative agreement with those in Ref. [40], we actually find noticeable quantitative differences, when resummed CP-violating self-energy and vertex effects are considered at the same time.

Next, we shall investigate numerically higher-order CP-violating vertex and self-energy effects induced by t and b- quarks on the electron EDM d_e. Fig. 5 shows numerical estimates for those resummed effects on d_e as functions of $\tan\beta$, in variants of the CPX scenario, with (a) $M_{H^+} = 150$ GeV and (b) $M_{H^+} = 300$ GeV. In particular, we considered three different choices of the gluino phase: $\arg(m_{\tilde{g}}) = 90°,\ 0,\ -90°$, denoted as $t_{1,2,3}$, respectively. We find that CP-violating threshold corrections to the $H_i tt$-coupling as small as 5% are sufficient to lead to observable EDM values for d_e. In this respect, we see that the t-quark effects strongly depend on the gluino phase through the combination $\mathrm{Im}\,(\mu m_{\tilde{g}})$ that occurs in $\mathrm{Im}\,(\Delta h_t/h_t)$ [cf. (A.4), (A.5)]. Thus, t-quark contribution to d_e is positive (negative) for negative (positive) gluino phases, while it is one-order of magnitude smaller and negative for vanishing gluino phases, i.e. for $\arg(m_{\tilde{g}}) = 0°$. For comparison, we also include in Fig. 5 the dependence of positive stop/sbottom contributions to d_e [2] (long-dash-dotted lines) on $\tan\beta$. The sum of the t, b- quark and $\tilde{t}, \tilde{b}$- squark contributions to d_e is given by the solid lines $1, 2, 3$ for the same values of gluino phases. As before, we indicate negative contributions to d_e with a minus sign. From Figs. 5(a) and (b), it is interesting to notice that if $\arg(m_{\tilde{g}}) = 90°$ in CPX, a cancellation between the t-quark and $\tilde{t}$-squark EDM contributions occurs for almost the entire range of the perturbatively allowed $\tan\beta$ values and for all phenomenologically viable charged Higgs-boson masses.

As a consequence of such a cancellation, the electron EDM d_e is always smaller than the current 2σ-experimental limit on d_e, i.e. $d_e < 2. \times 10^{-27}$ e cm, even for large $\tan\beta$ values up to 30. As we will see below, this prediction may considerably change if contributions from the CP-violating operator C_S or chargino two-loop effects are considered.

In order to further gauge the importance of the t-quark two-loop EDM effects, we present in Fig. 6 numerical values for d_e versus the μ-parameter for $\tan\beta = 20$, and for two charged Higgs-boson masses: (a) $M_{H^+} = 150$ GeV and (b) $M_{H^+} = 300$ GeV. The soft-SUSY breaking parameters are chosen as given in (4.1) for $M_{\rm SUSY} = 1$ TeV, except for the μ-parameter which has been varied from 0.1–4 TeV. For the sake of comparison, we also included the Higgs-boson two-loop EDM effects induced by $\tilde{t}$ and $\tilde{b}$ squarks. The meaning of the various types of lines is exactly the same as those in Fig. 5. Remarkably enough, we find that even μ values as low as 500 GeV may be sufficient to lead to an electron EDM at the observable level through the original two-loop Barr-Zee graph in Fig. 2(c). In this context, we also observe that the resummed Higgs-boson two-loop contributions to d_e from t-quarks are comparable and even larger than those coming from $\tilde{t}$-squarks for maximal gluino phases. In fact, if $A_{t,b} = 0$, the $\tilde{t}$-squark and dominant CP-violating Higgs-mixing effects may be completely switched off, without affecting much the corresponding t-quark two-loop contributions to d_e. Note that in this case the t-quark effects on d_e and the b-quark effects on the C_S operator, which both formally arise at the two-loop level, are proportional to $\mathrm{Im}\,(\mu m_{\tilde{g}})$. Therefore, they turn out to be strongly correlated and their combined contribution to $d_{\rm Tl}$ should carefully be taken into account (see also discussions of Figs. 8 and 9 below).

As has already been pointed out in [2, 3], charginos might also contribute to electron EDM d_e at the two-loop level. Recently, a computation of those effects appeared in [41]. The authors derived strict constraints on the CP-violating parameters of a scenario in which electroweak baryogenesis is mediated by CP-violating currents involving chargino interactions. Here, we re-examine this issue within a scenario that favours the above mechanism of electroweak baryogenesis and is not in conflict with LEP2 limits on the Higgs-boson masses and couplings. Specifically, being conservative, we require that it is $M_{H_i} \gtrsim 111$ GeV, for $g^2_{H_iZZ} \gtrsim 0.3$, where g_{H_iZZ} is the H_iZZ-coupling given in units of the SM $h_{\rm SM}ZZ$-coupling. In addition, we demand that $M_{H_i} + M_{H_j} \gtrsim 170$ GeV. On the other hand, in order that electroweak baryogenesis proceeds via a sufficiently strong first-order phase transition, the right-handed stop mass parameter $\widetilde{M}_t$ must be rather small, and the μ and the soft gaugino parameter $m_{\widetilde{W}}$ must not be too large, typically smaller than 0.5 TeV [13, 14]. Especially, there is a resonant enhancement even up to 10 times the observed baryon asymmetry, if the condition $\mu = m_{\widetilde{W}}$ is met [14]. Further requirements for a scenario leading to successful electroweak baryogenesis are: (i) a moderate trilinear A_t-parameter in the range, $0.2 \lesssim A_t/\widetilde{M}_Q \lesssim 0.65$; (ii) a not very large $\tan\beta$ value, $\tan\beta \lesssim 20$; (iii) a soft-SUSY breaking parameter $\widetilde{M}_Q$ of a few TeV, for phenomenological reasons [14]. More explicitly, the following values for the mass parameters are employed:

$$
\begin{aligned}
\widetilde{M}_Q &= 3\ \text{TeV}\,, \qquad \widetilde{M}_t \;=\; 0\,, \qquad \widetilde{M}_b \;=\; 3\ \text{TeV}\,, \\
|A_t| &= |A_b| \;=\; 1.8\ \text{TeV}\,, \qquad \arg(A_{t,b}) \;=\; 0^\circ\,, \qquad \tan\beta \;\lesssim\; 20\,, \\
|m_{\tilde{g}}| &= 3\ \text{TeV}\,, \qquad \arg(m_{\tilde{g}}) \;=\; 0^\circ\,, \\
\mu &= |m_{\widetilde{W}}| \;\lesssim\; 0.5\ \text{TeV}\,, \qquad \arg(m_{\widetilde{W}}) = 90^\circ\,.
\end{aligned}
\tag{4.2}
$$

To be able to compare our predictions with those presented in Fig. 2 of Ref. [41], we choose in Fig. 7(a) the values: $\mu = m_{\widetilde{W}} = 0.2$ TeV and $M_{H^+} = 170$ GeV. Since CP-violating Higgs-mixing effects in the mass spectrum are generically small for the chosen values of the parameters in (4.2), our mass input $M_{H^+} = 170$ GeV corresponds to $M_{`A'} \approx 150$ GeV for the mass of the almost CP-odd Higgs scalar A. Even though on a very qualitative basis our numerical results agree with those reported in [41] concerning the linear $\tan\beta$-increase behaviour of d_e, the actual functional dependences of the individual 'h', 'H', 'A' contributions to d_e on $\tan\beta$ differ significantly. Unlike [41], we find in Fig. 7(a) that for $\tan\beta \gtrsim 5$, the $\tan\beta$-enhanced effect on d_e originates from the heavier Higgs bosons 'H' and 'A', while the EDM contribution due to the lightest Higgs boson 'h' is almost negligible.[4] Since the size of d_e is set by the heavier Higgs-boson masses, i.e. by M_{H^+}, and by μ and $m_{\widetilde{W}}$, our predictions are rather robust under the different choices of the remaining soft-SUSY-breaking parameters. Moreover, although our numerical values for the total contribution to d_e agree very well with [41] for $\tan\beta = 2$ ($d_e \approx 0.63 \times 10^{-26}$ e cm), they are smaller by $\sim$20% for $\tan\beta = 6$, i.e. we find $d_e \approx 1.62 \times 10^{-26}$ e cm which should be compared with $d_e \approx 2. \times 10^{-26}$ e cm. Finally, the electroweak baryogenesis scenario (4.2) in the low $\tan\beta$ region, $\tan\beta \lesssim 6$, which is studied by the authors in [41], appears to be highly disfavoured by LEP2 data. In this respect, a phenomenologically viable model, with $M_{H^+} = 170$ GeV, would require larger values of $\tan\beta$, i.e. $\tan\beta \gtrsim 9$. In this case, one has to consider a factor of 10 suppression in the chargino phase, such that the chargino two-loop EDM effects are reduced to a level close to the experimental upper limit on d_e. Consequently, if no cancellations are assumed with possible one-loop EDM terms, then a model with suppressed chargino phase of $\sim 5^\circ$ and a relatively light charged Higgs boson, $M_{H^+} = 150$–200 GeV,

[4] The fact that only 'H' and 'A' contributions to d_e exhibit a linearly enhanced dependence on $\tan\beta$ may also be verified independently by a flavour-graph analysis.

might still be possible to account for the observed baryon asymmetry in the Universe, provided the aforementioned resonant factor 10 is to be used. However, the above situation may be considerably relaxed for larger values of M_{H^+}, since the chargino two-loop EDM effect on d_e decreases approximately as $1/M_{H^+}$ as M_{H^+} increases. This dependence of d_e on M_{H^+} can explicitly be seen in the lower panel (b) of Fig. 7, for increasing charged Higgs-boson masses: $M_{H^+} = 150$ GeV (solid), 200 GeV (dashed), 300 GeV (dotted), 500 GeV (dash-dotted) and 1 TeV (long-dash-dotted), in a scenario with $m_{\widetilde{W}} = \mu = 0.4$ TeV and $\arg(m_{\widetilde{W}}) = 90°$.

In the following, we will present predictions for more realistic EDM observables, with relatively reduced hadronic uncertainties, namely the thallium EDM $d_{\rm Tl}$, the neutron EDM d_n, as well as the muon EDM d_μ which was suggested to be measured with a high sensitivity to the level of 10^{-24} e cm [20]. In Fig. 8, we display numerical values for $d_{\rm Tl}$, d_n and d_μ as functions of $\tan\beta$ in two versions of the CPX scenario, with $M_{H^+} = 150$ GeV: (a) $\arg(m_{\tilde{g}}) = \arg(m_{\widetilde{W}}) = 90°$, and (b) $\arg(m_{\tilde{g}}) = 35°$, $\arg(m_{\widetilde{W}}) = 90°$. Fig. 8 also shows the different contributions, along with their relative signs, to $d_{\rm Tl}$ from top/stop (long-dash-dotted) and chargino (dotted) Higgs-boson two-loop graphs, as well as from the CP-odd electron-nucleon operator C_S (dashed). Note that the type of lines used to represent the numerical results of the individual EDM contributions is given in the parentheses. In the upper panel (a) of Fig. 8, we see that the contribution of C_S prevails in $d_{\rm Tl}$, for large values of $\tan\beta$, and exceeds the experimental limit, for $\tan\beta \gtrsim 12$. The prediction for d_n stays always below the current experimental limit, and the predicted values for d_μ do not reach the proposed experimental sensitivity for almost all relevant values of $\tan\beta$. It is amusing to remark that no EDM constraints can be imposed on the CPX scenario in the range: $4 \lesssim \tan\beta \lesssim 12$, which is interesting for analyzing Higgs-boson searches at high-energy colliders. In fact, if the gluino phase is chosen to be $\arg(m_{\tilde{g}}) = 35°$ (see Fig. 8(b)), the different EDM terms contributing to $d_{\rm Tl}$ approximately cancel and $d_{\rm Tl}$ does not exceed much the experimental limit. Similarly, since the top/stop- CEDM effects are small in this CPX scenario, the neutron EDM is always smaller than its conservative experimental upper bound: 1.2×10^{-25} e cm. However, for $\tan\beta \approx 40$, muon EDM can be significant, and its value $d_\mu \sim 4. \times 10^{-24}$ e cm lies well within the proposed explorable range. This example nicely illustrates the important rôle of complementarity of a high-sensitivity measurement of a muon EDM in constraining the CP-violating parameter space of the MSSM.

It is also interesting to examine the dependence of the different EDM contributions shown in Fig. 8 on the μ-parameter, for large values of $\tan\beta$. In Fig. 9, we display numerical values of $d_{\rm Tl}$, d_n and d_μ as functions of μ for two scenarios, with $\tan\beta = 40$, $M_{\rm SUSY} =$

1 TeV, $m_{\tilde{g}} = 1$ TeV, $m_{\widetilde{W}} = m_{\widetilde{B}} = 0.3$ TeV, $\arg(m_{\tilde{g}}) = \arg(m_{\widetilde{W}}) = 90°$, $A_{t,b} = 2$ TeV, $\arg(A_{t,b}) = 90°$: (a) $M_{H^+} = 150$ GeV; (b) $M_{H^+} = 300$ GeV. In analogy with Fig. 8, the individual contributions to $d_{\rm Tl}$ due to top/stop and chargino two-loop graphs and due to the CP-odd electron-nucleon operator C_S are also shown. In Fig. 9(a), we observe that the different CP-violating EDM operators may cancel in $d_{\rm Tl}$ and d_n, even for smaller values of the μ-parameter, i.e. for $\mu \approx 700$ GeV. In this region of parameter space, the muon EDM is predicted to be as large as 0.8×10^{-23} e cm, which falls within the reach of the proposed d_μ measurement. In Fig. 9(b), we give numerical estimates of $d_{\rm Tl}$, d_n and d_μ for a CPX scenario with a heavier charged Higgs boson, i.e. for $M_{H^+} = 300$ GeV. Again, we find that the predicted value for $d_{\rm Tl}$ can be close to the experimental limit for a wide range of μ-values, while d_μ always stays above the proposed experimental sensitivity.

Let us summarize the focal points of this section. We have explicitly demonstrated that the nonobservation of a thallium EDM can provide strict constraints on the CP-violating parameters related to third generation squarks, charginos and gluinos. The constraints derived from the neutron EDM limit are less restrictive. Nevertheless, our numerical analysis has also shown that the constraints from the thallium EDM can be significantly weakened, if the different CP-violating operators d_e and C_S cancel in $d_{\rm Tl}$. For instance, this could be the case for the benchmark scenario CPX, for low and intermediate values of $\tan\beta$. Such cancellations of the CP-violating operators d_e and C_S can occur for a wide range of parameters and crucially depend on the choice of the phase combinations: $\arg(\mu A_t)$, $\arg(\mu m_{\tilde{g}})$ and $\arg(\mu m_{\widetilde{W}})$. In particular, we find that a possible high-sensitivity measurement of d_μ to the proposed level of 10^{-24} e cm can constrain such uncovered ranges of CP-violating parameters in a rather complementary way. Finally, unless M_{H^+} is of order TeV, EDM constraints from $d_{\rm Tl}$ on scenarios favoured by electroweak baryogenesis are rather stringent. They generally imply either suppressed chargino phases, i.e. $\arg(m_{\widetilde{W}}) \lesssim 10°$, or modest cancellations in 1 part to 10 with one-loop EDM terms induced by the first two generations of sleptons.

5 Conclusions

To avoid the known CP and FCNC crises in the MSSM, we have considered a framework, in which the first two generation of squarks and sleptons are heavier than ~ 10 TeV, while the third generation is light, with masses not larger than TeV. Within this framework of the MSSM, we have performed a systematic study of the dominant two- and higher-loop contributions to the thallium, neutron and muon EDMs which are induced by b, t-quarks,

$\tilde{b}, \tilde{t}$-squarks, charginos and gluinos. At present, the most severe limits are obtained from the nonobservation of a thallium EDM d_{Tl}, whereas experimental upper limits on the neutron EDM d_n are less stringent and usually constrain large contributions from a d-quark CEDM and the CP-odd three-gluon operator. Also, theoretical predictions for d_n are plagued by a number of uncertainties while estimating hadronic matrix elements.

The largest effects on the thallium EDM d_{Tl} result from two operators, the CP-odd electron-nucleon operator C_S and the electron EDM d_e. These two CP-violating operators are formally induced at the two- and higher- loop levels and involve the exchange of CP-mixed Higgs bosons. Thus, strong constraints on the radiatively-generated CP-violating Higgs sector of the MSSM can be derived from d_{Tl}, and hence on the analyses for direct searches of CP-violating Higgs bosons at high-energy colliders, such as LEP2, Tevatron and LHC [44]. In this context, we have analyzed the compatibility of an earlier suggested benchmark scenario of maximal CP violation for LEP2 Higgs studies (CPX) [9] with the thallium and neutron EDMs. We have observed the existence of strong correlations among the different EDM terms which enable the suppression of d_{Tl} and d_n even below the present experimental limits. Specifically, for $4 \lesssim \tan\beta \lesssim 12$ in the CPX scenario with $M_{H^+} =$ 150 GeV, the stop, gluino, and chargino phases are all allowed to receive their maximal values, i.e. $\arg(A_t) = \arg(m_{\tilde{g}}) = \arg(m_{\widetilde{W}}) = 90^\circ$, without being in conflict with EDM limits (cf. Fig. 8(a)). Most interestingly, for specific choices of the gluino phase, the allowed range of $\tan\beta$ values compatible with EDM limits can be enlarged dramatically. For instance, if $\arg(m_{\tilde{g}}) = 35^\circ$ in the aforementioned CPX scenario (see also Fig. 8(b)), the predicted values for $25 \lesssim \tan\beta \lesssim 45$ do not contradict upper limits on thallium and neutron EDMs. For the remaining range of $\tan\beta$ values, the obtained predictions are larger than the 2σ upper bound on $|d_{\mathrm{Tl}}|$ by a factor of few only. Evidently, the degree of cancellations required between the one- and two-loop EDM terms in the CPX scenario is not excessive, for certain choices of the gluino phase.

At this point, it is important to stress that a muon EDM d_μ measured at the 10^{-24} e cm-level will help to sensitively probe CP-violating regions of the MSSM parameter space which cannot be accessed easily by measurements of the thallium and neutron EDMs. This complementarity property is mainly a consequence of the fact that d_μ is free from interfering CP-odd electron-nucleus interactions due to the C_S operator which can contribute significantly to d_{Tl}. Unlike the neutron EDM d_n, d_μ does not suffer from hadronic uncertainties. Given the absence of a signal in the measurements of $|d_{\mathrm{Tl}}|$ and $|d_n|$, one may now wonder whether a positive signal in d_μ would already imply a positive signal on $g-2$ as well. This is not the case within our framework of the MSSM. If the first two generation of sfermions are above the TeV scale, the biggest contribution to $g-2$ comes again from related two-loop Barr-Zee-type graphs. However, for phenomenologically viable charged Higgs-boson masses $M_{H^+} \gtrsim 120$ GeV in the MSSM [43], these effects on $g-2$ are negligible [45]. Then, only post-LEP2 high-energy colliders and the proposed BNL experiment [20] on the muon EDM d_μ might be able to sensitively explore the CP-violating parameter space of the above framework of the MSSM in a rather complementary manner.

We have also studied the impact of EDM constraints on the mechanism of electroweak baryogenesis induced by CP-violating chargino currents. For this purpose, we considered a scenario in (4.2), which favours the above mechanism of electroweak baryogenesis [14]. In such a scenario, the chargino two-loop graphs of Fig. 2(d) represent the dominant contribution to d_e and $d_{\rm Tl}$ as well. However, as we detailed in Section 4, our theoretical predictions for d_e are at variance with those presented in a recent communication [41]. Moreover, we find that LEP2 direct limits on Higgs-boson masses require intermediate and larger values of $\tan\beta$, i.e. $\tan\beta \gtrsim 6$, for a phenomenologically viable scenario of electroweak baryogenesis. In this $\tan\beta$ regime, experimental upper limits on $|d_{\rm Tl}|$ give rise to strict constraints, especially when no cancellations between the chargino two-loop and one-loop EDM terms are assumed. In the latter case, the charged Higgs-boson mass M_{H^+} should be rather heavy, i.e. $M_{H^+} \gtrsim 700$ GeV for $\tan\beta \gtrsim 6$ and $\arg(m_{\widetilde{W}}) \lesssim 90^\circ$. Otherwise, for lighter charged Higgs bosons, either the chargino phase should be suppressed at least by a factor of 10 or cancellations in 1 part to 10 with one-loop EDM terms need be invoked.

In our computation of the Higgs-boson loop-induced EDMs, we have considered resummation effects of higher-order CP-conserving and CP-violating terms in Higgs-boson self-energies and vertices. In particular, the original t-quark two-loop graph suggested by Barr and Zee [4] occurs beyond the two-loop approximation through threshold effects in the $H_i\bar{t}t$-coupling and, depending on the choice of the gluino phase, it might even compete with the $\tilde{t}$-squark two-loop graph [2]. Since our resummation of higher-order terms relied on an effective Lagrangian approach, one may worry about the relevance of other higher-order terms present in a complete computation. At this stage, we can only offer estimates of those possible higher-order electroweak uncertainties in the calculation of EDMs. Thus, we have checked our results with and without resumming the Higgs-boson self-energies. In this way, no large modifications are found in our predictions; the variation of our results is generally less than 10% for $M_{H^+} \lesssim 170$ GeV, and becomes even smaller to less than 1% for $M_{H^+} \gtrsim 200$ GeV. This may be attributed to the fact that the dominant contributions to EDMs come from the heaviest Higgs bosons on which the relative impact of radiative effects is less important. On the other hand, CP-violating threshold effects constitute the main source of theoretical uncertainties in the calculation of the original Barr-Zee graph of Fig. 2(c), as they are less controllable for low values of $\tan\beta$.[5] In this context, we remark that even the computation of the CP-odd three-gluon operator is haunted by relevant higher-order electroweak uncertainties in the MSSM [30]. The Weinberg operator can be generated in its original fashion [29] at three and higher loops which involve CP-violating self-energy and vertex sub-graphs of Higgs bosons. It appears then necessary to develop improved techniques that would enable us to provide accurate estimates of (resummed) higher-order terms in the calculation of EDMs. The present work is a step towards to this direction.

Acknowledgements

The author thanks Marcela Carena and Carlos Wagner for discussions on issues related to electroweak baryogenesis, Adam Ritz for comments on the computation of the mercury EDM, Maxim Pospelov for clarifying remarks pertinent to [40], Darwin Chang and Wai-Yee Keung for communications with regard to [41], and Athanasios Dedes for critical remarks. Finally, the author thanks the CERN Theory Group for warm hospitality and support.

[5] A crude estimate suggests that these additional higher-order effects are smaller than 20%.

A Effective Higgs-boson couplings

A key rôle in our calculations plays the coupling of the CP-mixed Higgs bosons $H_{1,2,3}$ to t-, b-quarks, $\tilde{t}$-, $\tilde{b}$-squarks and charginos χ^+. In this appendix we present the effective Lagrangians describing the above interactions, after including dominant one- and two-loop CP-even/CP-odd quantum effects on the Higgs-boson masses and their respective mixings.

Following the conventions of [8], we first write down the effective Lagrangian of the Higgs-boson couplings to top- and bottom-quarks

$$\mathcal{L}_{H\bar{q}q} \;=\; -\sum_{i=1}^{3} H_i \left[\frac{g_w m_b}{2M_W}\, \bar{b} \left(g^S_{H_i bb} \,+\, i g^P_{H_i bb}\gamma_5 \right) b \,+\, \frac{g_w m_t}{2M_W}\, \bar{t} \left(g^S_{H_i tt} \,+\, i g^P_{H_i tt}\gamma_5 \right) t \right], \tag{A.1}$$

with [8]

$$\begin{aligned}
g^S_{H_i bb} \;&=\; \mathrm{Re}\left[\frac{1 \,+\, (\delta h_b/h_b)}{1 \,+\, (\delta h_b/h_b) \,+\, (\Delta h_b/h_b)\tan\beta} \right] \frac{O_{1i}}{\cos\beta} \\
&\quad + \mathrm{Re}\left[\frac{(\Delta h_b/h_b)}{1 \,+\, (\delta h_b/h_b) \,+\, (\Delta h_b/h_b)\tan\beta} \right] \frac{O_{2i}}{\cos\beta} \\
&\quad + \mathrm{Im}\left[\frac{(\Delta h_b/h_b)\,(\tan^2\beta \,+\, 1)}{1 \,+\, (\delta h_b/h_b) \,+\, (\Delta h_b/h_b)\tan\beta} \right] O_{3i}\,, && \text{(A.2)} \\
g^P_{H_i bb} \;&=\; -\,\mathrm{Re}\left\{ \frac{[1 \,+\, (\delta h_b/h_b)]\,\tan\beta \,+\, (\Delta h_b/h_b)}{1 \,+\, (\delta h_b/h_b) \,+\, (\Delta h_b/h_b)\tan\beta} \right\} O_{3i} \\
&\quad + \mathrm{Im}\left[\frac{(\Delta h_b/h_b)\,\tan\beta}{1 \,+\, (\delta h_b/h_b) \,+\, (\Delta h_b/h_b)\tan\beta} \right] \frac{O_{1i}}{\cos\beta} \\
&\quad - \mathrm{Im}\left[\frac{(\Delta h_b/h_b)}{1 \,+\, (\delta h_b/h_b) \,+\, (\Delta h_b/h_b)\tan\beta} \right] \frac{O_{2i}}{\cos\beta}\,, && \text{(A.3)} \\
g^S_{H_i tt} \;&=\; \mathrm{Re}\left[\frac{1 \,+\, (\delta h_t/h_t)}{1 \,+\, (\delta h_t/h_t) \,+\, (\Delta h_t/h_t)\cot\beta} \right] \frac{O_{2i}}{\sin\beta} \\
&\quad + \mathrm{Re}\left[\frac{(\Delta h_t/h_t)}{1 \,+\, (\delta h_t/h_t) \,+\, (\Delta h_t/h_t)\cot\beta} \right] \frac{O_{1i}}{\sin\beta} \\
&\quad + \mathrm{Im}\left[\frac{(\Delta h_t/h_t)\,(\cot^2\beta \,+\, 1)}{1 \,+\, (\delta h_t/h_t) \,+\, (\Delta h_t/h_t)\cot\beta} \right] O_{3i}\,, && \text{(A.4)} \\
g^P_{H_i tt} \;&=\; -\,\mathrm{Re}\left\{ \frac{[1 \,+\, (\delta h_t/h_t)]\,\cot\beta \,+\, (\Delta h_t/h_t)}{1 \,+\, (\delta h_t/h_t) \,+\, (\Delta h_t/h_t)\cot\beta} \right\} O_{3i} \\
&\quad + \mathrm{Im}\left[\frac{(\Delta h_t/h_t)\,\cot\beta}{1 \,+\, (\delta h_t/h_t) \,+\, (\Delta h_t/h_t)\cot\beta} \right] \frac{O_{2i}}{\sin\beta} \\
&\quad - \mathrm{Im}\left[\frac{(\Delta h_t/h_t)}{1 \,+\, (\delta h_t/h_t) \,+\, (\Delta h_t/h_t)\cot\beta} \right] \frac{O_{1i}}{\sin\beta}\,. && \text{(A.5)}
\end{aligned}$$

In (A.2)–(A.5), O is a 3×3-dimensional mixing matrix that relates weak to mass eigenstates of Higgs bosons in the presence of CP violation [6, 8], and $\delta h_{t,b}/h_{t,b}$ and $\Delta h_{t,b}/h_{t,b}$ represent

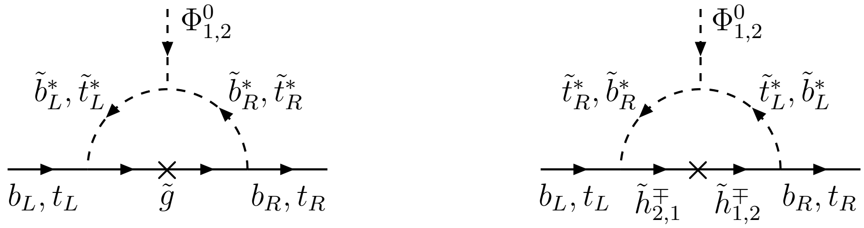

(a) **(b)**

Figure 3: *Effective one-loop $\Phi^0_{1,2}\bar{b}b$ and $\Phi^0_{1,2}\bar{t}t$ couplings, $\delta h_{b,t}$ and $\Delta h_{b,t}$, generated by the exchange of (a) gluinos $\tilde{g}$ and (b) Higgsinos $\tilde{h}^\pm_{1,2}$.*

non-logarithmic threshold contributions to bottom and top Yukawa couplings [46]. As is shown in Fig. 3, the latter quantities are predominantly induced by gluino and Higgsino loops. In the presence of CP violation, their analytic forms are [8]

$$\frac{\delta h_b}{h_b} \;=\; -\frac{2\alpha_s}{3\pi} m^*_{\tilde{g}} A_b I(m^2_{\tilde{b}_1}, m^2_{\tilde{b}_2}, |m_{\tilde{g}}|^2) \;-\; \frac{|h_t|^2}{16\pi^2} |\mu|^2 I(m^2_{\tilde{t}_1}, m^2_{\tilde{t}_2}, |\mu|^2)\,, \tag{A.6}$$

$$\frac{\Delta h_b}{h_b} \;=\; \frac{2\alpha_s}{3\pi} m^*_{\tilde{g}} \mu^* I(m^2_{\tilde{b}_1}, m^2_{\tilde{b}_2}, |m_{\tilde{g}}|^2) \;+\; \frac{|h_t|^2}{16\pi^2} A^*_t \mu^* I(m^2_{\tilde{t}_1}, m^2_{\tilde{t}_2}, |\mu|^2)\,, \tag{A.7}$$

$$\frac{\Delta h_t}{h_t} \;=\; \frac{2\alpha_s}{3\pi} m^*_{\tilde{g}} \mu^* I(m^2_{\tilde{t}_1}, m^2_{\tilde{t}_2}, |m_{\tilde{g}}|^2) \;+\; \frac{|h_b|^2}{16\pi^2} A^*_b \mu^* I(m^2_{\tilde{b}_1}, m^2_{\tilde{b}_2}, |\mu|^2)\,, \tag{A.8}$$

$$\frac{\delta h_t}{h_t} \;=\; -\frac{2\alpha_s}{3\pi} m^*_{\tilde{g}} A_t I(m^2_{\tilde{t}_1}, m^2_{\tilde{t}_2}, |m_{\tilde{g}}|^2) \;-\; \frac{|h_b|^2}{16\pi^2} |\mu|^2 I(m^2_{\tilde{b}_1}, m^2_{\tilde{b}_2}, |\mu|^2)\,, \tag{A.9}$$

where $\alpha_s = g_s^2/(4\pi)$ is the $\mathrm{SU}(3)_c$ fine structure constant, and $I(a,b,c)$ is the one-loop function

$$I(a,b,c) \;=\; \frac{ab\ln(a/b) + bc\ln(b/c) + ac\ln(c/a)}{(a-b)(b-c)(a-c)}\;. \tag{A.10}$$

In addition, the stop and sbottom masses are given by (with $q = t, b$)

$$\begin{aligned} m^2_{\tilde{q}_1\,(\tilde{q}_2)} \;=\; \frac{1}{2}\bigg\{ & \widetilde{M}^2_Q \;+\; \widetilde{M}^2_q \;+\; 2\,m^2_q \;+\; T^q_z\, \cos 2\beta M^2_Z \\ & +(-)\sqrt{\Big[\,\widetilde{M}^2_Q - \widetilde{M}^2_q + \cos 2\beta M^2_Z\,(T^q_z - 2Q_q \sin^2\theta_w)\Big]^2 \;+\; 4\,m^2_q\,|A_q - R_q\mu^*|^2}\;\bigg\}\,, \end{aligned} \tag{A.11}$$

where $Q_t\,(Q_b) \;=\; 2/3\,(-1/3)$, $T^t_z \;=\; -T^b_z \;=\; 1/2$, $R_t\,(R_b) \;=\; \cot\beta\;(\tan\beta)$, and $\sin^2\theta_w \;=\; 1 - M^2_W/M^2_Z$.

It is important to remark here that only the CP-violating vertex effects on $g^S_{H_i bb}$ and $g^P_{H_i bb}$, which are proportional to $\mathrm{Im}\,[(\Delta h_b/h_b)\tan^2\beta]$ in (A.2) and (A.3), are enhanced for moderately large values of $\tan\beta$, i.e. $20 \lesssim \tan\beta \lesssim 40$. However, for very large values of $\tan\beta$, i.e. $\tan\beta \gtrsim 40$, there is a $1/\tan^2\beta$-dependent damping factor due to CP-violating resummation effects that cancels the $\tan^2\beta$-enhanced factor mentioned above. As a consequence, in the large $\tan\beta$ limit, the coupling factors $g^S_{H_ibb}$ and $g^P_{H_ibb}$ approach a $\tan\beta$-independent constant. Related discussion is also given in Section 2.

Another important ingredient for our computation of two-loop EDMs is the diagonal effective couplings of the Higgs bosons to scalar top- and bottom- quarks. Taking the CP-violating Higgs-mixing effects into account, the effective Lagrangian of interest to us may be conveniently written in the form

$$\mathcal{L}^{\rm diag}_{H\tilde{q}^*\tilde{q}} \;=\; \sum_{i=1}^{3} H_i \sum_{q=t,b} \Big[v\,\xi_q^{(H_i)} \Big(\tilde{q}_1^*\tilde{q}_1 \;-\; \tilde{q}_2^*\tilde{q}_2 \Big) \;+\; v\,\zeta_q^{(H_i)} \Big(\tilde{q}_1^*\tilde{q}_1 \;+\; \tilde{q}_2^*\tilde{q}_2 \Big) \Big]\,, \tag{A.12}$$

where

$$\xi_t^{(H_i)} \;=\; \frac{2m_t^2}{v^2\,(m^2_{\tilde{t}_2} \;-\; m^2_{\tilde{t}_1})} \Big[{\rm Im}\,(\mu A_t)\,\frac{O_{3i}}{\sin^2\beta} \;-\; {\rm Re}\,(\mu X_t)\,\frac{O_{1i}}{\sin\beta} \;+\; {\rm Re}\,(A_t^* X_t)\,\frac{O_{2i}}{\sin\beta} \Big]\,, \tag{A.13}$$

$$\xi_b^{(H_i)} \;=\; \frac{2m_b^2}{v^2\,(m^2_{\tilde{b}_2} - m^2_{\tilde{b}_1})} \Big[{\rm Im}\,(\mu A_b)\,\frac{O_{3i}}{\cos^2\beta} \;-\; {\rm Re}\,(\mu X_b)\,\frac{O_{2i}}{\cos\beta} \;+\; {\rm Re}\,(A_b^* X_b)\,\frac{O_{1i}}{\cos\beta} \Big]\,, \tag{A.14}$$

$$\zeta_t^{(H_i)} \;=\; -\,\frac{2m_t^2}{v^2}\,\frac{O_{2i}}{\sin\beta} \;+\; \mathcal{O}(g_w^2, g'^2)\,, \qquad \zeta_b^{(H_i)} \;=\; -\,\frac{2m_b^2}{v^2}\,\frac{O_{1i}}{\cos\beta} \;+\; \mathcal{O}(g_w^2, g'^2)\,, \tag{A.15}$$

with $X_q = A_q - R_q\mu^*$ $(q = t, b)$. Although we assumed $m^2_{\tilde{q}_1} > m^2_{\tilde{q}_2}$, the effective Lagrangian (A.12) exhibits the nice feature that it is fully independent of the hierarchy of the squark masses.

Finally, we present the effective couplings of the CP-mixed Higgs bosons $H_{1,2,3}$ to charginos $\chi^+_{1,2}$ [7, 47]. These may be conveniently described by the effective Lagrangian

$$\mathcal{L}_{H\chi^+\chi^-} \;=\; -\,\frac{g_w}{2\sqrt{2}} \sum_{i=1}^{3} H_i \sum_{j,k=1,2} \bar{\chi}_j^+ \Big(a_{H_i\chi_j^-\chi_k^+} \;+\; b_{H_i\chi_j^-\chi_k^+}\, i\gamma_5 \Big)\, \chi_k^+\,, \tag{A.16}$$

where

$$\begin{aligned} a_{H_i\chi_j^-\chi_k^+} \;=\;& O_{1i}\Big(C^{R*}_{2j}\,C^L_{1k} \;+\; C^R_{2k}\,C^{L*}_{1j} \Big) \;+\; O_{2i}\Big(C^{R*}_{1j}\,C^L_{2k} \;+\; C^R_{1k}\,C^{L*}_{2j} \Big) \\ & -\,i\,O_{3i}\Big[\sin\beta\Big(C^{R*}_{2j}\,C^L_{1k} \;-\; C^R_{2k}\,C^{L*}_{1j} \Big) \;+\; \cos\beta\Big(C^{R*}_{1j}\,C^L_{2k} \;-\; C^R_{1k}\,C^{L*}_{2j} \Big) \Big]\,, \end{aligned} \tag{A.17}$$

$$\begin{aligned} b_{H_i\chi_j^-\chi_k^+} \;=\;& i\,O_{1i}\Big(C^{R*}_{2j}\,C^L_{1k} \;-\; C^R_{2k}\,C^{L*}_{1j} \Big) \;+\; i\,O_{2i}\Big(C^{R*}_{1j}\,C^L_{2k} \;-\; C^R_{1k}\,C^{L*}_{2j} \Big) \\ & +\,O_{3i}\Big[\sin\beta\Big(C^{R*}_{2j}\,C^L_{1k} \;+\; C^R_{2k}\,C^{L*}_{1j} \Big) \;+\; \cos\beta\Big(C^{R*}_{1j}\,C^L_{2k} \;+\; C^R_{1k}\,C^{L*}_{2j} \Big) \Big]\,. \end{aligned} \tag{A.18}$$

In the above, C^R and C^L are 2×2 unitary matrices which diagonalize the chargino mass matrix,

$$M_C \ = \ \left(\begin{array}{cc} m_{\widetilde{W}} & g_w\langle\phi_2^{0*}\rangle \\ g_w\langle\phi_1^0\rangle & \mu \end{array} \right)\,, \tag{A.19}$$

with $\langle\phi_1^0\rangle = v_1/\sqrt{2}$ and $\langle\phi_2^{0*}\rangle = v_2/\sqrt{2}$, through the bi-unitary transformation

$$C^{R\dagger} M_C\, C^L \ = \ \mathrm{diag}\left(m_{\chi_1^+},\ m_{\chi_2^+}\right)\,. \tag{A.20}$$

In (A.20), the chargino mass-eigenvalues are given by

$$\begin{aligned} m_{\chi_1^+(\chi_2^+)} \ &= \ \frac{1}{2}\Big[\,|m^2_{\widetilde{W}}|\ +\ |\mu|^2\ +\ 2M_W^2 \\ &\quad -(+)\ \sqrt{(|m^2_{\widetilde{W}}| + |\mu|^2 + 2M_W^2)^2\ -\ 4\,|m_{\widetilde{W}}\mu\ -\ M_W^2\sin 2\beta|^2}\ \Big]\,, \end{aligned} \tag{A.21}$$

while the analytic expressions for the mixing matrices $C^{L,R}$ are quite lengthy in the presence of CP violation, and will not be presented here; they can be computed using standard techniques [7].

For completeness, we give the corresponding effective couplings of the would-be Goldstone boson G^0 to charginos $\chi^+_{1,2}$:

$$\begin{aligned} a_{G^0\chi_j^-\chi_k^+} \ &= \ i\,\cos\beta\left(C^{R*}_{2j}\,C^L_{1k}\ -\ C^R_{2k}\,C^{L*}_{1j}\right)\ -\ i\,\sin\beta\left(C^{R*}_{1j}\,C^L_{2k}\ -\ C^R_{1k}\,C^{L*}_{2j}\right)\,, \\ b_{G^0\chi_j^-\chi_k^+} \ &= \ -\,\cos\beta\left(C^{R*}_{2j}\,C^L_{1k}\ +\ C^R_{2k}\,C^{L*}_{1j}\right)\ +\ \sin\beta\left(C^{R*}_{1j}\,C^L_{2k}\ +\ C^R_{1k}\,C^{L*}_{2j}\right)\,. \end{aligned} \tag{A.22}$$

A non-trivial consistency check for the correctness of our analytic results is the vanishing of the diagonal scalar couplings of the G^0 boson to charginos, i.e. $a_{G^0\chi_j^-\chi_j^+} = 0$.

References

[1] G.F. Giudice and S. Dimopoulos, Phys. Lett. **B357** (1995) 573; G. Dvali and A. Pomarol, Phys. Rev. Lett. **77** (1996) 3728; A.G. Cohen, D.B. Kaplan, and A.E. Nelson, Phys. Lett. **B388** (1996) 588; P. Binétruy and E. Dudas, Phys. Lett. **B389** (1996) 503.

[2] D. Chang, W.-Y. Keung and A. Pilaftsis, Phys. Rev. Lett. **82** (1999) 900 and **83** (1999) 3972 (E).

[3] A. Pilaftsis, Phys. Lett. **B471** (1999) 174; D. Chang, W.-F. Chang and W.-Y. Keung, Phys. Lett. **B478** (2000) 239.

[4] S.M. Barr and A. Zee, Phys. Rev. Lett. **65** (1990) 21.

[5] A. Pilaftsis, Phys. Rev. **D58** (1998) 096010 and Phys. Lett. **B435** (1998) 88.

[6] A. Pilaftsis and C.E.M. Wagner, Nucl. Phys. **B553** (1999) 3; D.A. Demir, Phys. Rev. **D60** (1999) 055006; S.Y. Choi, M. Drees and J.S. Lee, Phys. Lett. **B481** (2000) 57; G.L. Kane, L.-T. Wang, Phys. Lett. **B488** (2000) 383; S.Y. Choi, K. Hagiwara and J.S. Lee, Phys. Rev. **D64** (2001) 032004; Phys. Lett. **B529** (2002) 212, S. Heinemeyer, Eur. Phys. J. **C22** (2001) 521; T. Ibrahim and P. Nath, hep-ph/0204092; S.W. Ham, S.K. Oh, E.J. Yoo, C.M. Kim and D. Son, hep-ph/0205244.

[7] T. Ibrahim and P. Nath, Phys. Rev. **D63** (2001) 035009.

[8] M. Carena, J. Ellis, A. Pilaftsis and C.E.M. Wagner, Nucl. Phys. **B586** (2000) 92.

[9] M. Carena, J. Ellis, A. Pilaftsis and C.E.M. Wagner, Phys. Lett. **B495** (2000) 155.

[10] M. Carena, J. Ellis, A. Pilaftsis and C.E.M. Wagner, Nucl. Phys. **B625** (2002) 345.

[11] For phenomenological applications of radiative Higgs-sector CP violation in the MSSM, see: S.Y. Choi and M. Drees, Phys. Rev. Lett. **81** (1998) 5509; S. Baek and P. Ko, Phys. Rev. Lett. **83** (1999) 488; W. Bernreuther, A. Brandenburg and M. Flesch, hep-ph/9812387; K.S. Babu, C. Kolda, J. March-Russell and F. Wilczek, Phys. Rev. **D59** (1999) 016004; B. Grzadkowski, J.F. Gunion and J. Kalinowski, Phys. Rev. **D60** (1999) 075011; S.Y. Choi, M. Guchait, H.S. Song and W.Y. Song, Phys. Lett. **B483** (2000) 168; P. Osland, Acta Phys. Polon. **B30** (1999) 1967; T. Han, T. Huang, Z.H. Lin, J.X. Wang and X. Zhang, Phys. Rev. **D61** (2000) 015006; B. Grzadkowski and

J. Pliszka, Phys. Rev. **D60** (1999) 115018; S.Y. Choi and J.S. Lee, Phys. Rev. **D61** (2000) 015003; C.-S. Huang and L. Wei, Phys. Rev. **D61** (2000) 116002; K. Freese and P. Gondolo, hep-ph/9908390; S.Y. Choi and J.S. Lee, Phys. Rev. **D61** (2000) 115002; A. Dedes and S. Moretti, Phys. Rev. Lett. **84** (2000) 22; Nucl. Phys. **B576** (2000) 29; M.S. Berger, Phys. Rev. Lett. **87** (2001) 131801; D.A. Demir, Nucl. Phys. Proc. Suppl. **101** (2001) 431; S.W. Ham, S.K. Oh, E.J. Yoo and H.K. Lee, J. Phys. **G27** (2001) 1; M. Boz and N.K. Pak, Phys. Rev. **D65** (2002) 075014; A. Arhrib, D.K. Ghosh and O.C.W. Kong, Phys. Lett. **B537** (2002) 217; E. Christova, S. Fichtinger, S. Kraml and W. Majerotto, Phys. Rev. **D65** (2002) 094002; hep-ph/0205227; C.-H. Chen, hep-ph/0206143; M.N. Dubinin and A.V. Semenov, hep-ph/0206205; A. Bartl, K. Hidaka, T. Kernreiter and W. Porod, hep-ph/0207186.

[12] V.A. Kuzmin, V.A. Rubakov and M.E. Shaposhnikov, Phys. Lett. **B155** (1985) 36.

[13] For recent studies, see: M. Carena, M. Quirós and C.E.M. Wagner, Nucl. Phys. **B524** (1998) 3; M. Laine and K. Rummukainen, Phys. Rev. Lett. **80** (1998) 5259; Nucl. Phys. **B535** (1998) 423; Nucl. Phys. **B597** (2001) 23; K. Funakubo, Prog. Theor. Phys. **102** (1999) 389; J. Grant and M. Hindmarsh, Phys. Rev. **D59** (1999) 116014; M. Losada, Nucl. Phys. **B537** (1999) 3; Nucl. Phys. **B569** (2000) 125; S. Davidson, M. Losada and A. Riotto, Phys. Rev. Lett. **84** (2000) 4284; A.B. Lahanas, V.C. Spanos and V. Zarikas, Phys. Lett. **B472** (2000) 119; N. Rius and V. Sanz, Nucl. Phys. **B570** (2000) 155; J.M. Cline, M. Joyce and K. Kainulainen, JHEP **0007** (2000) 018; [Erratum:hep-ph/0110031]; S.J. Huber, P. John and M.G. Schmidt, Eur. Phys. J. **C20** (2001) 695; H. Murayama and A. Pierce, hep-ph/0201261.

[14] M. Carena, J.M. Moreno, M. Quirós, M. Seco and C.E.M. Wagner, Nucl. Phys. **B599** (2001) 158; and work in progress.

[15] P.G. Harris et al., Phys. Rev. Lett. **82** (1999) 904.

[16] B.C. Regan, E.D. Commins, C.J. Schmidt and D. DeMille, Phys. Rev. Lett. **88** (2002) 071805.

[17] S. Barr, Phys. Rev. Lett. **68** (1992) 1822; Int. J. Mod. Phys. **A8** (1993) 209.

[18] W. Fischler, S. Paban and S. Thomas, Phys. Lett. **B289** (1992) 373.

[19] I.B. Khriplovich and S.K. Lamoreaux, *CP Violation Without Strangeness*, (Springer, New York, 1997).

[20] Y.K. Semertzidis et al., Letter of Intent to BNL (Spring of 2000, and Fall of 1997); "Sensitive Search for a Permanent Muon Electric Dipole Moment," [hep-ph/0012087]. For recent theoretical studies, see T. Ibrahim and P. Nath, Phys. Rev. **D64** (2001) 093002; J.L. Feng, K.T. Matchev and Y. Shadmi, Nucl. Phys. **B613** (2001) 366; J.R. Ellis, J. Hisano, M. Raidal and Y. Shimizu, Phys. Lett. **B528** (2002) 86.

[21] K.F. Smith et al., Phys. Lett. **B234** (1990) 191.

[22] P.G. Harris et al., Phys. Rev. Lett. **82** (1999) 904.

[23] S.K. Lamoreaux and R. Golub, Phys. Rev. **D61** (2000) 051301.

[24] M. Pospelov and A. Ritz, Phys. Rev. Lett. **83** (1999) 2526; Nucl. Phys. **B573** (2000) 177.

[25] S.A. Abel, S. Khalil and O. Lebedev, Nucl. Phys. **B606** (2001) 151.

[26] M.V. Romalis, W.C. Griffith and E.N. Fortson, Phys. Rev. Lett. **86** (2001) 2505.

[27] T. Falk, K.A. Olive, M. Pospelov and R. Roiban, Nucl. Phys. **B60** (1999) 3.

[28] A. Ritz, private communication.

[29] S. Weinberg, Phys. Rev. Lett. **63** (1989) 2333.

[30] J. Dai, H. Dykstra, R.G. Leigh, S. Paban, and D.A. Dicus, Phys. Lett. **B237** (1990) 216 and **B242** (1990) 547 (E).

[31] T. Ibrahim and P. Nath, Phys. Lett. **B418** (1998) 98, Phys. Rev. **D57** (1998) 478, **D58** (1998) 019901 (E), Phys. Rev. **D58** (1998) 111301; Phys. Rev. **D61** (2000) 093004; M. Brhlik, G.J. Good and G.L. Kane, Phys. Rev. **D59** (1999) 115004; M. Brhlik, L. Everett, G.L. Kane and J. Lykken, Phys. Rev. Lett. **83** (1999) 2124; Phys. Rev. **D62** (2000) 035005; S. Abel, S. Khalil and O. Lebedev, Phys. Rev. Lett. **86** (2001) 5850.

[32] J. Ellis, S. Ferrara and D.V. Nanopoulos, Phys. Lett. **B114** (1982) 231; W. Buchmüller and D. Wyler, Phys. Lett. **B121** (1983) 321; J. Polchinski and M. Wise, Phys. Lett. **B125** (1983) 393; F. del Aguila, M. Gavela, J. Grifols and A. Mendez, Phys. Lett. **B126** (1983) 71; D.V. Nanopoulos and M. Srednicki, Phys. Lett. **B128** (1983) 61; T. Falk, K.A. Olive and M. Srednicki, Phys. Lett. **B354** (1995) 99; M. Dugan, B. Grinstein and L. Hall, Nucl. Phys. **B255** (1985) 413; R. Garisto and J.D. Wells, Phys. Rev. **D55** (1997) 1611.

[33] P. Nath, Phys. Rev. Lett. **66** (1991) 2565; Y. Kizukuri and N. Oshimo, Phys. Rev. **D46** (1992) 3025.

[34] For recent analyses of one-loop EDM effects, see, S. Pokorski, J. Rosiek and C.A. Savoy, Nucl. Phys. **B570** (2000) 81; E. Accomando, R. Arnowitt and B. Dutta, Phys. Rev. **D61** (2000) 115003; A. Bartl, T. Gajdosik, W. Porod, P. Stockinger and H. Stremnitzer, Phys. Rev. **D60** (1999) 073003.

[35] In this respect, our analysis of EDM constraints on a CP-violating MSSM Higgs sector is complementary to the one presented by T. Ibrahim, Phys. Rev. **D64** (2001) 035009.

[36] A. Pilaftsis, Phys. Rev. **D62** (2000) 016007.

[37] T.H. West, Phys. Rev. **D50** (1994) 7; T. Kadoyoshi and N. Oshimo, Phys. Rev. **D55** (1997) 1481.

[38] In our numerical analysis, we employ the Fortran code `cph+.f` available at `http://home.cern.ch/p/pilaftsi/www/`. The code is based on a recent RG-improved diagrammatic calculation of Higgs-boson pole masses in the MSSM with explicit CP violation [10].

[39] For recent two-loop studies of an effective CP-conserving Higgs potential in the MSSM, see: M. Carena, H.E. Haber, S. Heinemeyer, W. Hollik, C.E.M. Wagner and G. Weiglein, Nucl. Phys. **B580** (2000) 29; J.R. Espinosa and R.J. Zhang, JHEP **0003** (2000) 026; M. Carena, S. Mrenna and C.E.M. Wagner, Phys. Rev. **D62** (2000) 055008; J.R. Espinosa and I. Navarro, Nucl. Phys. **B615** (2001) 82; A. Brignole, G. Degrassi, P. Slavich and F. Zwirner, Nucl. Phys. **B631** (2002) 195; hep-ph/0206101; S.P. Martin, hep-ph/0206136.

[40] O. Lebedev and M. Pospelov, hep-ph/0204359.

[41] D. Chang, W.-F. Chang and W.-Y. Keung, hep-ph/0205084 [v2, 4 June 2002].

[42] M.A. Shifman, A.L. Vainshtein and V.I. Zakharov, Phys. Lett. **B78** (1978) 443; see, also, J. Ellis, M.K. Gaillard and D.V. Nanopoulos, Nucl. Phys. **B106** (1976) 292; S. Dawson and H.E. Haber, Int. J. Mod. Phys. **A7** (1992) 107.

[43] OPAL Collaboration, "Interpretation of the Search for Neutral Higgs Bosons from $\sqrt{s} = 91$ GeV to $\sqrt{s} = 209$ GeV in a CP-Violating MSSM Scenario," OPAL Physics Note PN505, available from `http://opal.web.cern.ch/Opal/pubs/physnote/html/pn505.html`.

[44] M. Carena, J. Ellis, S. Mrenna, A. Pilaftsis and C.E.M. Wagner, work in progress.

[45] D. Chang, W.-F. Chang, C.-H. Chou and W.-Y. Keung, Phys. Rev. **D63** (2001) 091301; A. Dedes and H.E. Haber, JHEP **0105** (2001) 006.

[46] E. Ma, Phys. Rev. **D39** (1989) 1922; R. Hempfling, Phys. Rev. **D49** (1994) 6168; L.J. Hall, R. Rattazzi and U. Sarid, Phys. Rev. **D50** (1994) 7048; T. Blazek, S. Raby and S. Pokorski, Phys. Rev. **D52** (1995) 4151; M. Carena, M. Olechowski, S. Pokorski and C.E.M. Wagner, Nucl. Phys. **B426** (1994) 269; S. Heinemeyer, W. Hollik and G. Weiglein, Phys. Lett. **B440** (1998) 296; Eur. Phys. J. **C9** (1999) 343; F. Borzumatti, G. Farrar, N. Polonsky and S. Thomas, Nucl. Phys. **B555** (1999) 53; J.R. Espinosa and R.J. Zhang, Nucl. Phys. **B586** (2000) 3.

[47] S.Y. Choi, M. Drees, J.S. Lee and J. Song, hep-ph/0204200.

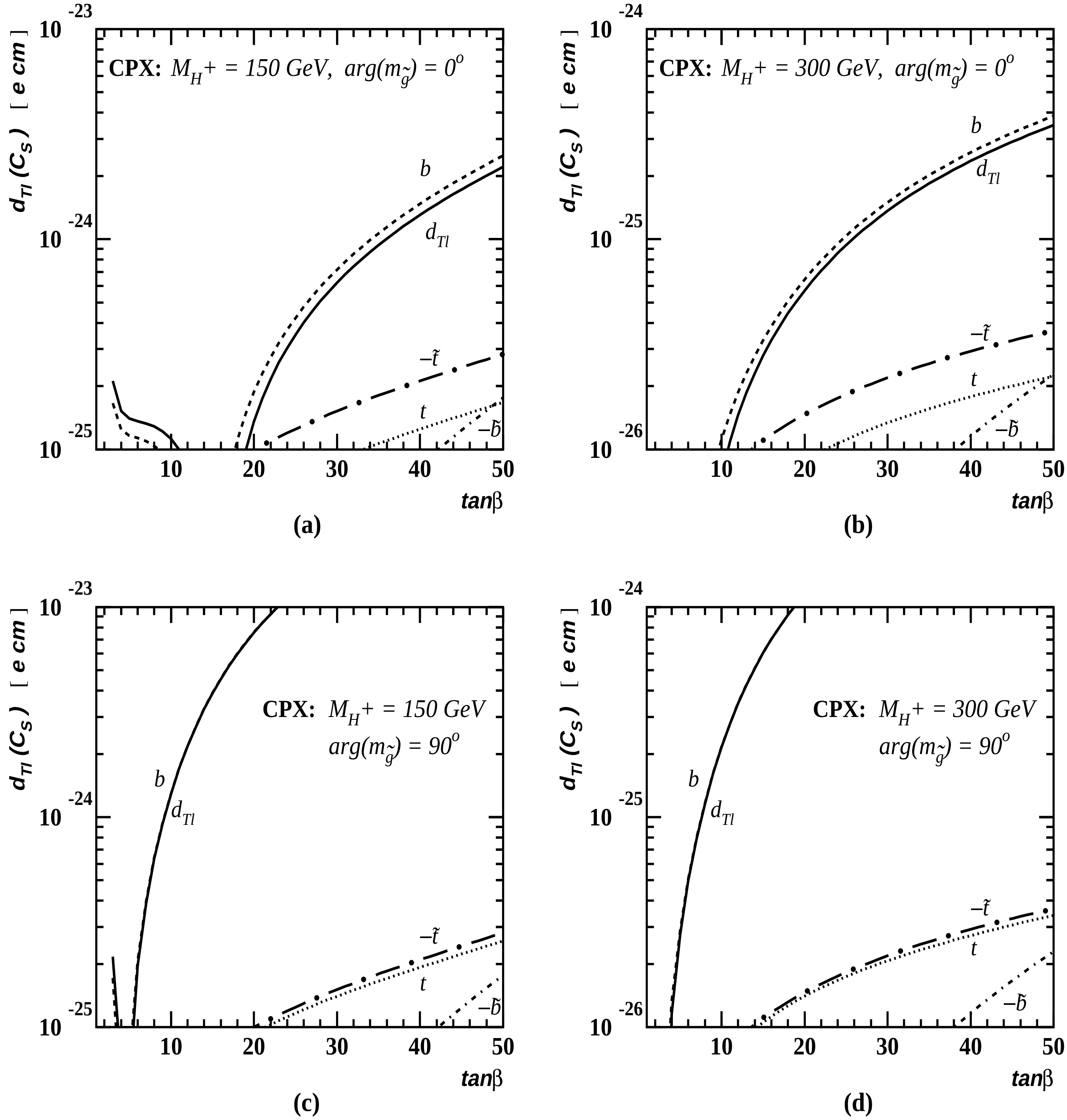

Figure 4: *Numerical estimates of* ^{205}*Tl EDM* $d_{\rm Tl}$ *induced by the CP-odd electron-nucleon operator* C_S *as functions of* $\tan\beta$*, in four selected CPX scenarios with* $M_{\rm SUSY} = 1$ *TeV. The values of the CPX parameters are given in (4.1). The individual* $b, \tilde{t}, t, \tilde{b}$ *contributions to* $d_{\rm Tl}(C_S)$*, along with their relative signs, are also displayed.*

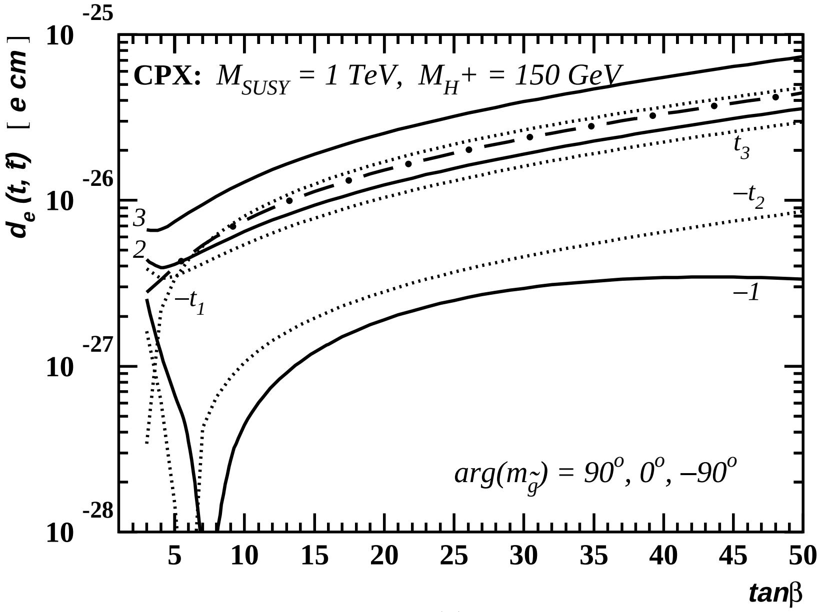

(a)

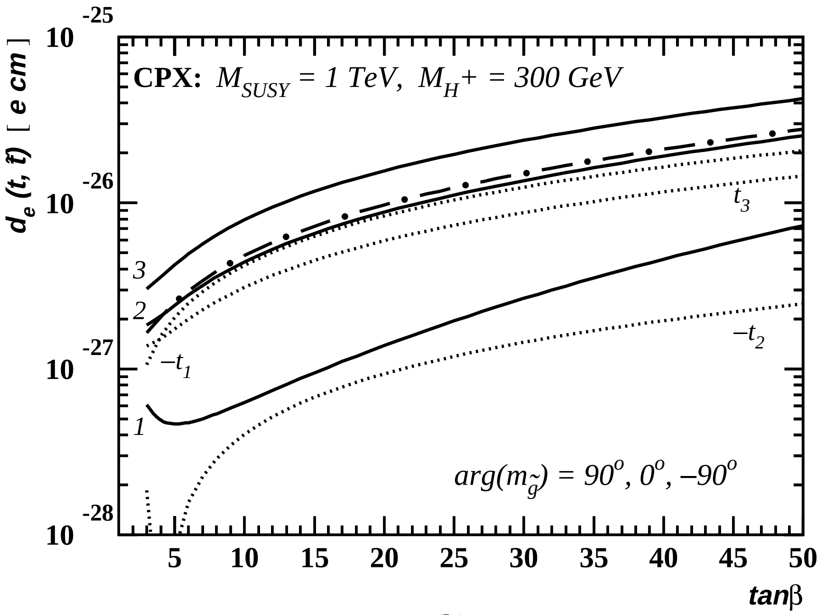

(b)

Figure 5: *Numerical estimates of resummed Higgs-boson two-loop effects on d_e, induced by t, b- quarks and $\tilde{t}, \tilde{b}$- squarks, as functions of $\tan\beta$, in two variants of the CPX scenario, with (a) $M_{H^+} = 150$ GeV and (b) $M_{H^+} = 300$ GeV. The long-dash-dotted lines indicate the stop/sbottom contributions to d_e. The dotted lines $t_{1,2,3}$ correspond to top/bottom contributions, for $\arg(m_{\tilde{g}}) = 90^\circ,\ 0^\circ,\ -90^\circ$, respectively. Likewise, the solid lines $1, 2, 3$ give the sum of all the aforementioned contributions to d_e for the same values of gluino phases. Negative contributions to d_e are denoted with a minus sign.*

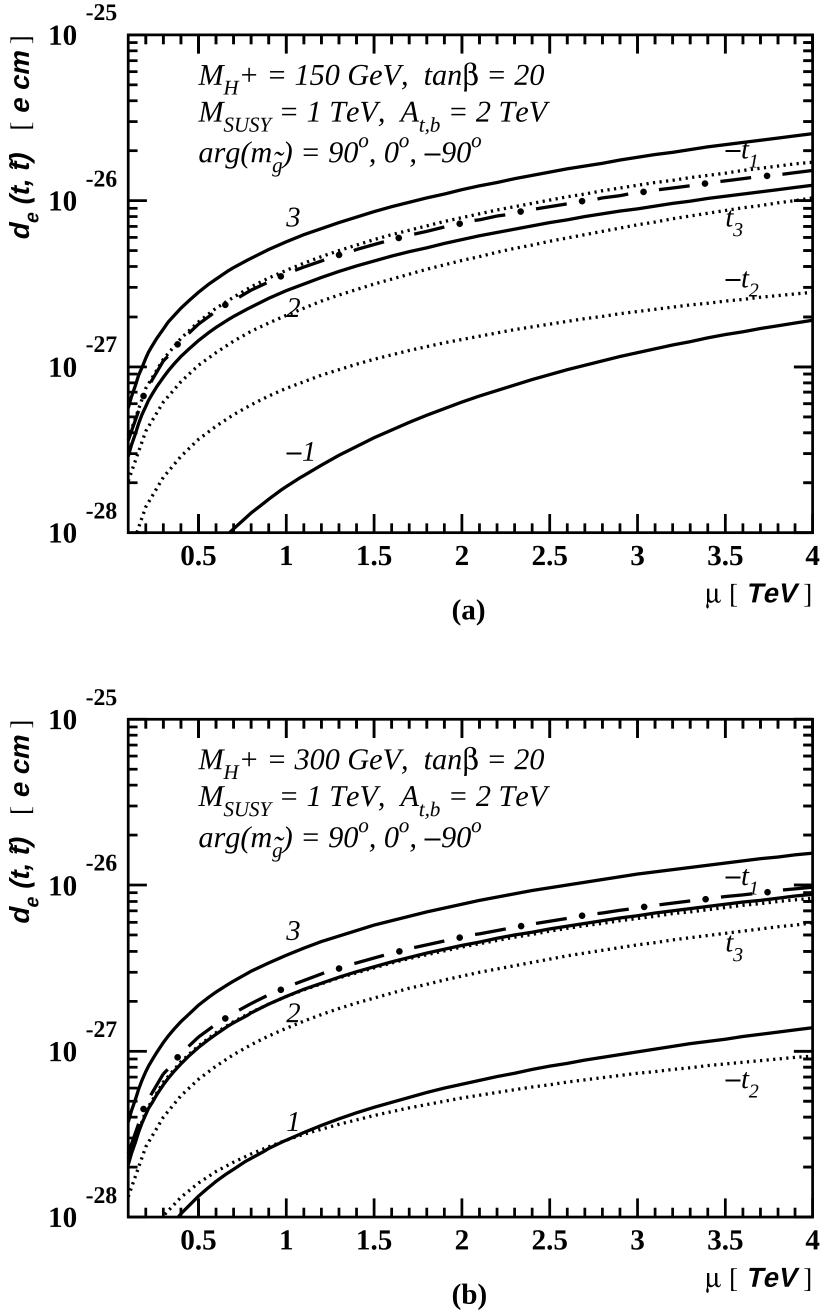

Figure 6: *Numerical values of resummed Higgs-boson two-loop effects on d_e, induced by t, b- quarks and $\tilde{t}, \tilde{b}$- squarks, as functions of μ, in two variants of the CPX scenario, with* $\tan\beta = 20$, *and (a)* $M_{H^+} = 150$ *GeV and (b)* $M_{H^+} = 300$ *GeV. The meaning of the different line types is indentical to that of Fig. 5. For* $A_{t,b} = 0$, *the long-dash-dotted line disappears and so the solid lines collapse to the dotted ones.*

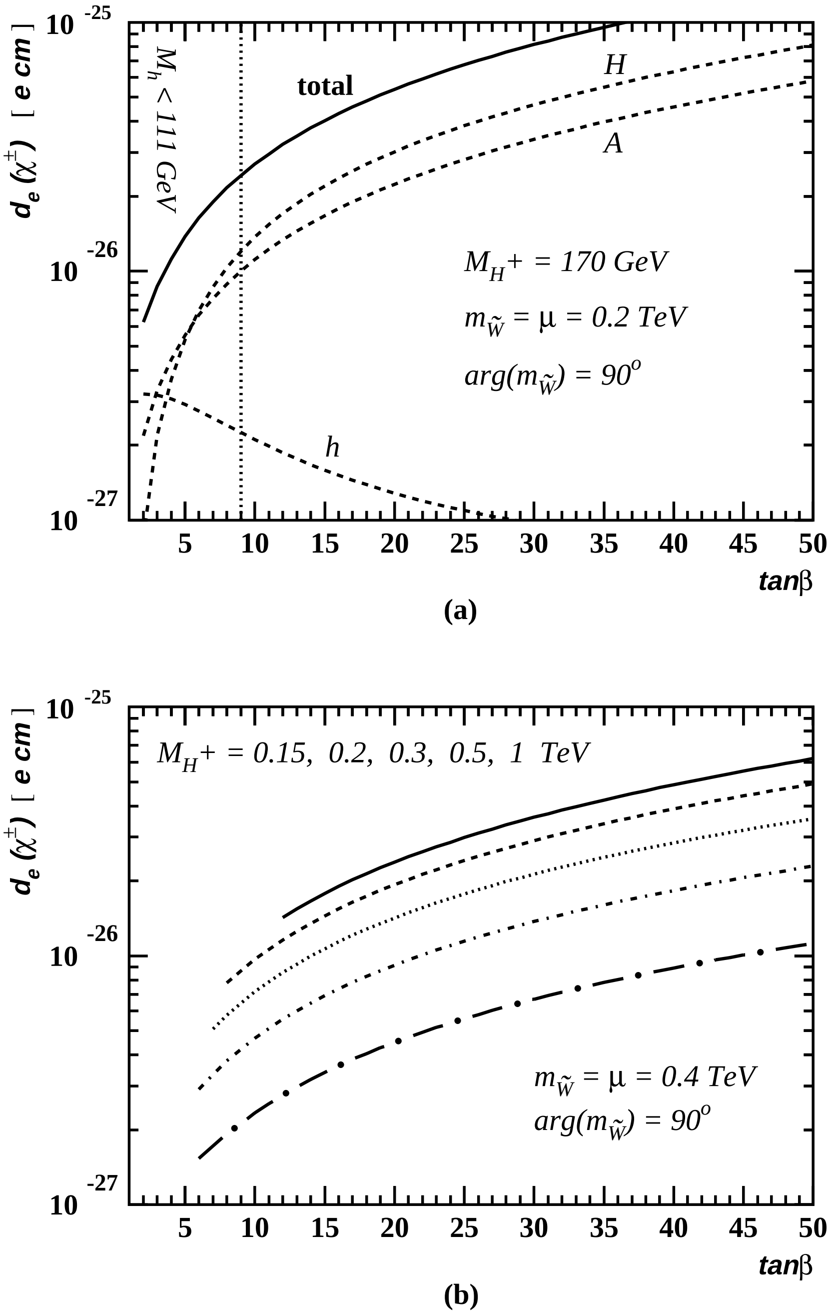

Figure 7: *d_e versus* $\tan\beta$ *in a scenario favoured by electroweak baryogenesis, with MSSM parameters* $\widetilde{M}_Q = \widetilde{M}_D = 3$ *TeV,* $\widetilde{M}_U = 0$*,* $A_{t,b} = 1.8$ *TeV,* $m_{\tilde{g}} = 3$ *TeV and* $\arg(A_{t,b}) = \arg(m_{\tilde{g}}) = 0°$*. In the upper panel (a),* $M_{H^+} = 170$ *GeV is used, corresponding to* $M_{\text{‘}A\text{’}} \approx 150$ *GeV, and* $m_{\widetilde{W}} = \mu = 0.2$ *TeV and* $\arg(m_{\widetilde{W}}) = 90°$*. Also displayed are the individual ‘h’, ‘H’, ‘A’ contributions to* d_e *and the LEP excluded region from direct Higgs-boson searches. In the lower panel (b), numerical values are shown for* $M_{H^+} = 150$ *GeV (solid), 200 GeV (dashed), 300 GeV (dotted), 500 GeV (dash-dotted) and 1 TeV (long-dash-dotted), in a scenario with* $m_{\widetilde{W}} = \mu = 0.4$ *TeV and* $\arg(m_{\widetilde{W}}) = 90°$*.*

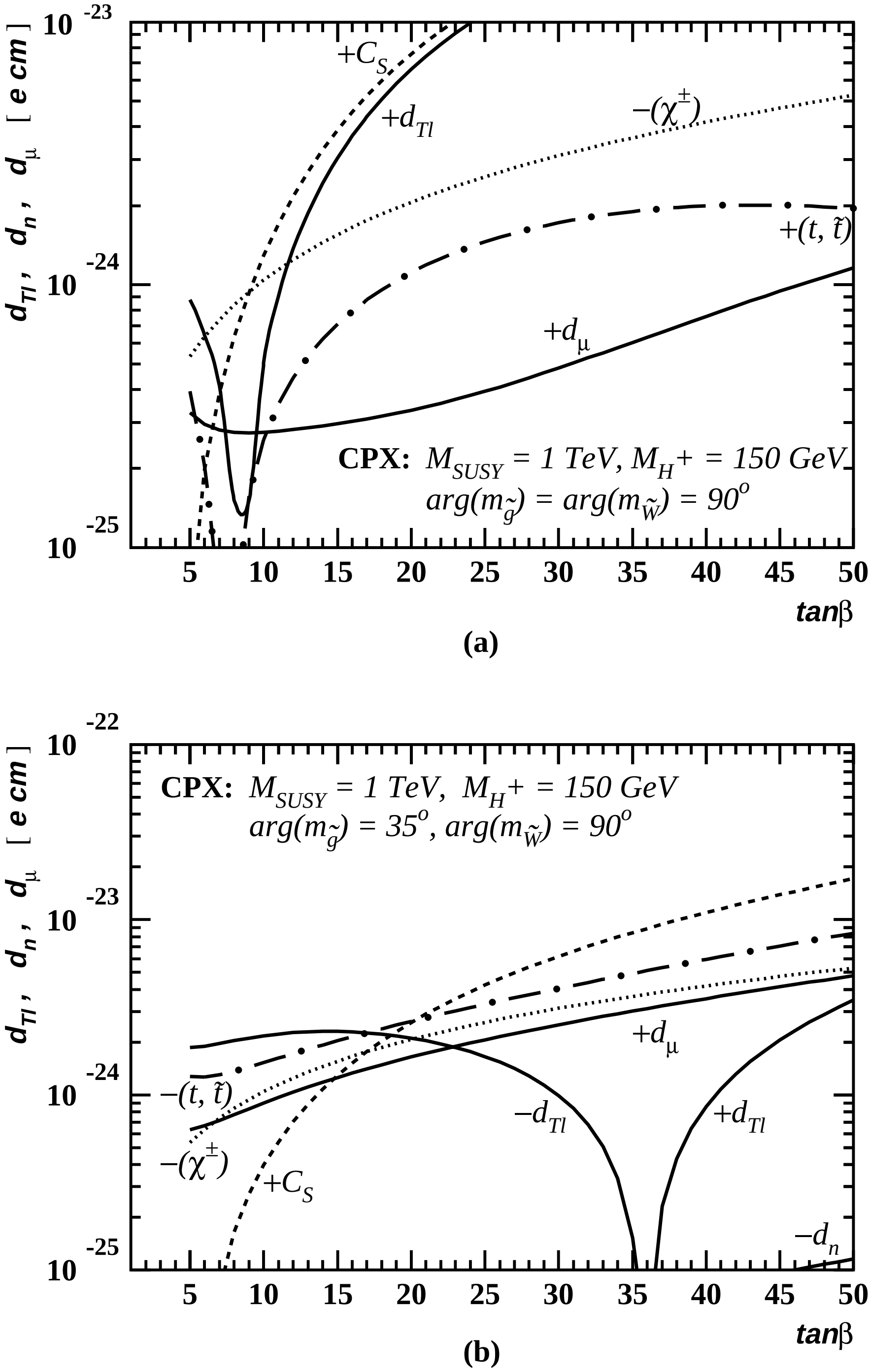

Figure 8: *EDMs of d_{Tl}, d_n and d_μ as functions of $\tan\beta$ in two versions of the CPX scenario: (a) $\arg(m_{\tilde{g}}) = \arg(m_{\widetilde{W}}) = 90^\circ$, and (b) $\arg(m_{\tilde{g}}) = 35^\circ$, $\arg(m_{\widetilde{W}}) = 90^\circ$. Also shown are the different contributions, along with their relative signs, to d_{Tl} from top/stop (long-dash-dotted) and chargino (dotted) Higgs-boson two-loop graphs, as well as from the CP-odd electron-nucleon coupling C_S (dashed).*

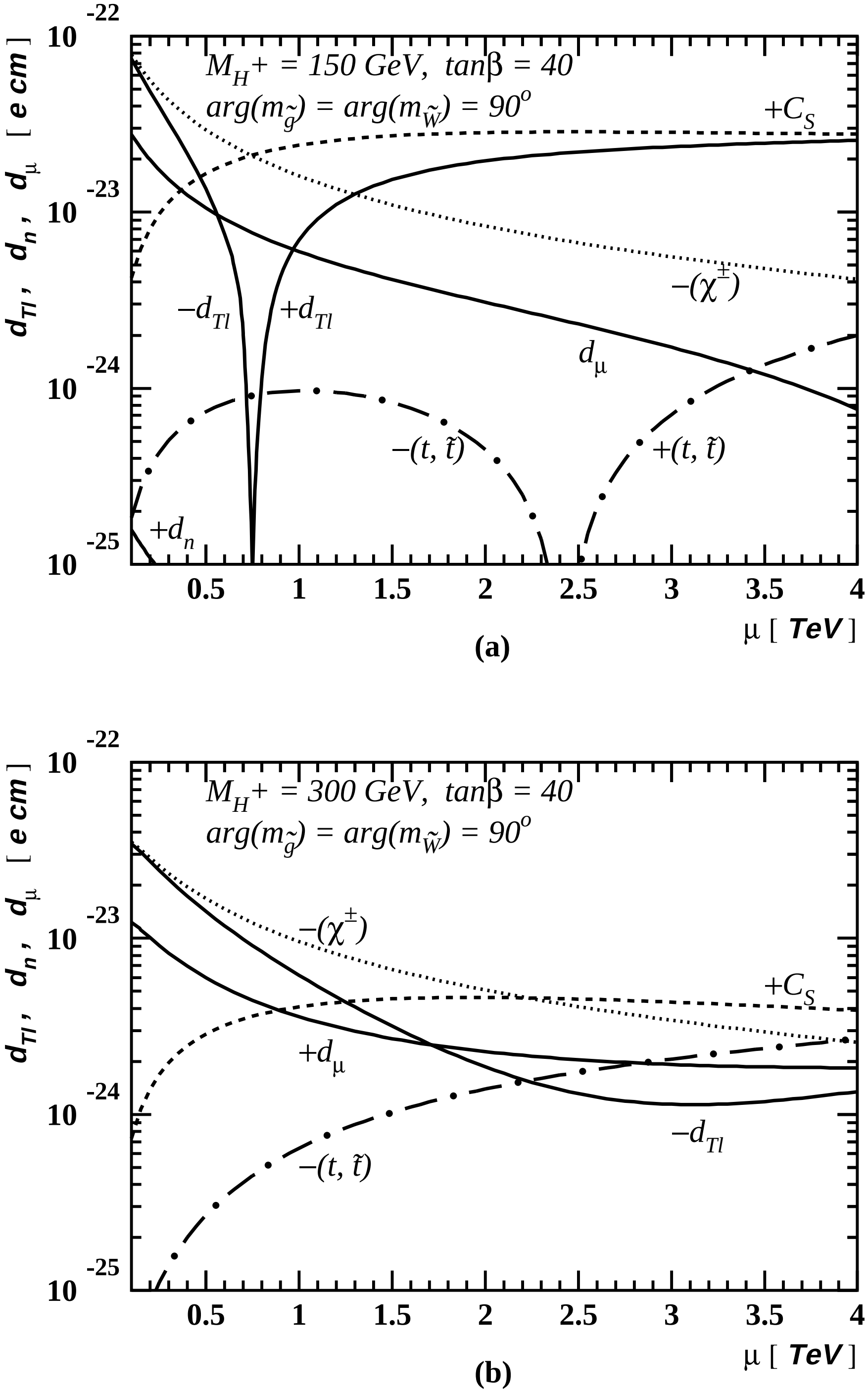

Figure 9: *Numerical values of* $d_{\rm Tl}$, d_n *and* d_μ *as functions of* μ *for two large-*$\tan\beta$ *scenarios, with* $\tan\beta = 40$, $M_{\rm SUSY} = 1$ *TeV,* $m_{\tilde{g}} = 1$ *TeV,* $m_{\widetilde{W}} = m_{\widetilde{B}} = 0.3$ *TeV,* $\arg(m_{\tilde{g}}) = \arg(m_{\widetilde{W}}) = 90^\circ$, $A_{t,b} = 2$ *TeV,* $\arg(A_{t,b}) = 90^\circ$*: (a)* $M_{H^+} = 150$ *GeV; (b)* $M_{H^+} = 300$ *GeV. In analogy with Fig. 8, the individual contributions to* $d_{\rm Tl}$ *due to top/stop and chargino two loop graphs and due to the* C_S *operator are also shown.*